NOTCH1 mutations associate with low CD20 level in chronic lymphocytic leukemia: evidence for a NOTCH1 mutation-driven epigenetic dysregulation

NOTCH1 mutations associate with low CD20 level in chronic lymphocytic leukemia: evidence for a *NOTCH1* mutation-driven epigenetic dysregulation

Federico Pozzo[1], Tamara Bittolo[1], Francesca Arruga[2], Pietro Bulian[1], Paolo Macor[3], Erika Tissino[1], Branimir Gizdic[2], Francesca Maria Rossi[1], Riccardo Bomben[1], Antonella Zucchetto[1], Dania Benedetti[1], Massimo Degan[1], Giovanni D'Arena[4], Annalisa Chiarenza[5], Francesco Zaja[6], Gabriele Pozzato[7], Davide Rossi[8], Gianluca Gaidano[8], Giovanni Del Poeta[9], Silvia Deaglio[2,10], Valter Gattei[1,11], Michele Dal Bo[1,11].

[1] Clinical and Experimental Onco-Hematology Unit, Centro di Riferimento Oncologico, I.R.C.C.S., Aviano (PN), Italy;
[2] Immunogenetics Unit, Human Genetics Foundation (HuGeF), Torino, Italy;
[3] Department of Life Sciences, University of Trieste, Trieste, Italy;
[4] Onco-Hematology Department, Centro di Riferimento Oncologico della Basilicata, I.R.C.C.S., Rionero in Vulture, Italy;
[5] Division of Hematology, Ferrarotto Hospital, Catania, Italy;
[6] Clinica Ematologica, Centro Trapianti e Terapie Cellulari "Carlo Melzi" DISM, Azienda Ospedaliera Universitaria S. Maria Misericordia, Udine, Italy;
[7] Department of Internal Medicine and Hematology, Maggiore General Hospital, University of Trieste, Trieste, Italy;
[8] Division of Hematology–Department of Translational Medicine –Amedeo Avogadro University of Eastern Piedmont, Novara, Italy.
[9] Division of Hematology, S. Eugenio Hospital and University of Tor Vergata, Rome, Italy;
[10] Department of Medical Sciences, University of Torino, Italy.

[11] VG and MDB equally contributed as senior authors

Correspondence**:** Michele Dal Bo, PhD, or Valter Gattei, MD,
Clinical and Experimental Onco-Hematology Unit, Centro di Riferimento Oncologico, I.R.C.C.S.,
Via Franco Gallini 2, postal code 33081, Aviano (PN), Italy
Tel: 0039-0434-659718
Tel: 0039-0434-659410
Fax: 0039-0434-659409
e-mail: mdalbo@cro.it;vgattei@cro.it

Running title: *NOTCH1* mutations and CD20 expression in CLL

Conflict of interest: the Authors declare no competing financial interests.

Abstract

In chronic lymphocytic leukemia (CLL), *NOTCH1* mutations have been associated with clinical resistance to the anti-CD20 rituximab, although the mechanisms behind this peculiar behavior remain to be clarified. In a wide CLL series (n=692), we demonstrated that CLL cells from *NOTCH1* mutated cases (87/692) were characterized by lower CD20 expression, and lower relative lysis induced by anti-CD20 exposure in-vitro. Consistently, CD20 expression by CLL cells was up-regulated in-vitro by γ-secretase inhibitors or NOTCH1-specific siRNA, and the stable transfection of a mutated (c.7541-7542delCT) NOTCH1 intracellular domain (NICD-mut) into CLL-like cells resulted in a strong downregulation of both CD20 protein and transcript. By using these NICD-mut transfectants, we investigated protein interactions of RBPJ, a transcription factor acting either as activator or repressor of NOTCH1 pathway when respectively bound to NICD or hystone deacetylases (HDACs). Compared to controls, NICD-mut transfectants had RBPJ preferentially complexed to NICD, and showed higher levels of HDACs interacting with the promoter of the CD20 gene. Finally, treatment with the HDAC inhibitor valproic acid upregulated CD20 in both NICD-mut transfectants and primary CLL cells. In conclusion, *NOTCH1* mutations are associated with low CD20 levels in CLL and are responsible for a dysregulation of HDAC-mediated epigenetic repression of CD20 expression.

Introduction

Chronic lymphocytic leukemia (CLL) is a heterogeneous disease with highly variable clinical courses and survivals ranging from months to decades. In particular, a subset of CLL patients is known to experience a progressive symptomatic disease poorly responsive to the common immuno-chemotherapeutic regimens.[1,2] A fraction of these high risk CLL, overall accounting for 5-10% of cases, can be identified by screening for *TP53* mutation/deletion,[1,2] while an additional fraction of cases has been recently shown to bear mutations involving the *NOTCH1*, *SF3B1* and *BIRC3* genes. Overall, alterations of these genes occur in approximately 20% of CLL patients at diagnosis and have significant correlations with survival in consecutive series from independent institutions.[3-7]

Mutations of *NOTCH1* are found in about 10% of CLL cases at diagnosis, with frequency increasing in advanced disease phases, in chemorefractory patients, and during transformation to Richter Syndrome.[3-5,7,8] Moreover, *NOTCH1* mutations are enriched in CLL patient subgroups defined by trisomy 12 and an unmutated *IGHV* gene status.[9,10] *NOTCH1* encodes for a transmembrane receptor acting as a ligand-activated transcription factor.[11,12] In particular, NOTCH1 signaling initiates when the ligand, from either the JAGGED or DELTA families, binds to the receptor and induces successive proteolytic cleavages, resulting in the release and nuclear translocation of the NOTCH1 intra-cellular domain (NICD). In the nucleus, the NICD becomes part of an activation complex along with the transcription factor RBPJ, that leads to the de-repression/activation of specific target genes, including genes of the HES family.[13-20] At variance with normal B cells, CLL cells constitutively express the NOTCH1 receptor as well as its ligands JAGGED1 and JAGGED2, suggesting autocrine/paracrine loops for NOTCH1 signaling activation.[21] In CLL, virtually all NOTCH1 mutations are frameshift or non-sense events clustering within exon 34, including a highly recurrent c.7541-7542delCT frameshift deletion, represented in 80% of cases.[3,4,10] These mutations result in the truncation of the C-PEST regulatory domain of the protein and the subsequent impaired degradation of the NICD,[3,4,22-24] which in turn determines to an intense and sustained activation of the NOTCH1 pathway.[25]

Recently, the presence of *NOTCH1* mutations has been associated with a relative resistance to anti-CD20 immunotherapy in a prospective clinical study comparing the effectiveness of the fludarabine plus cyclophosphamide (FC) regimen versus the FC plus rituximab (FCR) regimen[26], although the biological mechanisms underlying the differential activity of rituximab in relation to *NOTCH1* mutational status is still to be elucidated.

Materials and Methods

Primary cells from CLL patients and healthy donors

The study was approved by the Internal Review Board of the Aviano Centro di Riferimento Oncologico (Approval n. IRB-05-2010), and included peripheral blood samples from 692 patients with CLL.[27] Informed consent was obtained in accordance with the declaration of Helsinki. CLL cases were characterized for *IGHV* mutational status, the main cytogenetic abnormalities, CD38, CD49d, ZAP70 expression, as described.[28]

Primary CLL cells and normal B cells from healthy donors (n=3) were obtained from peripheral blood samples by Ficoll-Hypaque (Pharmacia, Uppsala, Sweden) density gradient centrifugation and used either directly or cryopreserved until use. All studies were performed on highly purified cells (>95% pure), as results of negative selection by immunomagnetic beads when required.[29] In-vitro studies were performed in CLL cells from *NOTCH1* mutated cases with relevant *NOTCH1* mutational burden, i.e >25% of total DNA, or in *NOTCH1* wild type cases, as control.

CD20 expression

CD20 expression was evaluated by flow cytometry at the Clinical and Experimental Onco-Hematology Unit (CRO, Aviano), in the 692 CLL cases entering this study, as part of the routine diagnostic procedures for CLL assessment. In particular, 495 cases were evaluated by a FITC-conjugated anti-CD20 antibody, while, in the remaining 197 cases, a PE-Cy7-conjugated antibody was employed (clone L27, in both cases, BD Biosciences, Milan, Italy), due to a modification of the flow cytometry diagnostic panel. For CD20 expression analyses, these two cohorts were kept separated. All experiments were performed on FACSCanto II (BD Biosciences, Milan, Italy).[28,29]

NOTCH1 mutational status

The presence of c.7541-7542delCT *NOTCH1* mutation was investigated by amplification refractory mutation system (ARMS) PCR, as described.[3,8,10] The load of c.7541-7542delCT *NOTCH1* mutation was evaluated by next generation sequencing (NGS) using a MiSeq sequencer (Illumina, San Diego, CA), with a ~1000X coverage-fold.

The presence of *NOTCH1* mutations other than the c.7541-7542delCT was investigated by Sanger sequencing in the entire *NOTCH1* PEST domain, as reported.[30] The mutational load was roughly determined (about 50%, 25-50%, about 25%, <25% of mutated DNA) by visual inspection of sequence electropherograms, as reported.[31]

Cell Sorting

CLL cells from selected *NOTCH1* mutated cases were sorted according to CD20 expression by using the PE-conjugated anti-CD20 antibody (BD Biosciences). The $CD20^{low}$ or $CD20^{high}$ fractions were selected below the 25^{th} percentile or above the 75^{th} percentile of CD20 expression, respectively. After CDC assay, CLL cells from selected *NOTCH1* mutated cases were sorted according to 7-aminoactinomycin (7-AAD, BD Biosciences) expression. Viable cell fraction was identified as 7-AAD-negative. Sorting was performed utilizing a FACSAriaIII cell sorter (BD Biosciences), as described.[29]

NICD plasmids and transfection

NICD Plasmids were engineered cloning the NICD coding sequence in a pcDNA3.1-NT-GFP-TOPO vector (Life Technologies, Monza, Italy). The c.7541-7542delCT mutation (NICD-mut) or c.5304G>A (NICD-null) mutation were inserted with the Quikchange II XL Mutagenesis kit

(Agilent, Milan, Italy). MEC-1 cells were transfected with the Amaxa Nucleofector (Lonza, Basel, Switzerland).

Primary CLL cells were transfected with siRNA for NOTCH1 (TriFECTa, RNAi kit, IDT, Leuven, Belgium) using the Amaxa Nucleofector, as reported.[32] NOTCH1 protein expression was evaluated by flow cytometry using the PE-conjugated anti-NOTCH1 antibody (clone MHN1-519, BD Biosciences).

Co-immunoprecipitation experiments

Nuclear extracts were obtained as reported.[33] Co-immunoprecipitation was performed using anti-RBPJ (clone ab25949, Abcam) and isotype (Millipore, Milan, Italy) antibodies. WB was performed using anti-NOTCH1 (D1E11, CST), anti-HDAC1 (10E2, Abcam), anti-HDAC2 (HDAC2-62, Abcam), anti-RBPJ (D10A4, CST) antibodies. Anti-ERK 1/2 (BD Biosciences) and anti-BRG1 (Santa Cruz Biotechnology, Heidelberg, Germany) were used as loading controls for cytoplasmic and nuclear lysates.

Chromatin immunoprecipitation (ChIP) assay

ChIP assays were performed with SimpleChIP enzymatic Chromatin IP kit (CST), according to standard manufacturer's protocol, using anti-HDAC1 (10E2, Abcam), anti-HDAC2 (HDAC2-62, Abcam), anti-Hystone H3 (kit provided) or control isotype (kit provided) antibodies. Qualitative PCR amplification of *MS4A1* promoter was performed as reported.[34] Quantification of *MS4A1* promoter DNA was determined by QRT-PCR.

Further details regarding the methods and the statistical approaches are provided as Supplementary Information.

Results

NOTCH1 mutational status and NOTCH1 protein expression in CLL

The presence of the c.7541-7542delCT *NOTCH1* mutation was investigated by ARMS PCR in 692 CLL cases. With this approach, the c.7541-7542delCT was detected in 81 cases (Table S1). Additional 6 cases with a *NOTCH1* mutation other than the c.7541-7542delCT were detected by Sanger sequencing (Table S1). Overall considered, *NOTCH1* mutated (*NOTCH1*-mut) cases represented about the 12% (i.e. 87/692 cases) of the cohort, in keeping with previous studies.[3-5] A quantitative detection of the c.7541-7542delCT was performed by NGS. As shown in Table S2, the *NOTCH1* mutational load ranged from 1% to 50% of total DNA, in agreement with the heterozygous nature of *NOTCH1* mutations and with its subclonal representation in some instances.[3-5]

NOTCH1 protein expression was evaluated by WB in *NOTCH1*-mut cases, chosen among those with high mutational load (i.e. > 25% of *NOTCH1* mutated DNA) and, for comparison, in *NOTCH1* wild type (*NOTCH1*-wt) CLL. In keeping with the presence of the c.7541-7542delCT that generates truncated protein with impaired degradation,[35] *NOTCH1*-mut cases showed high transmembrane NOTCH1 and NICD levels, both with molecular weights consistent with the truncation of the *NOTCH1* mutated protein (Figure S1).[4,21,25] Conversely, *NOTCH1*-wt CLL, although expressing discrete amount of transmembrane NOTCH1 in some instances, usually expressed less NICD protein than *NOTCH1*-mut cases (Figure S1).[4,21,25]

Correlation between CD20 expression and *NOTCH1* mutational status in CLL

CD20 expression was investigated by flow cytometry using either a FITC- or a PE-Cy7-conjugated antibody (Table S1), and separately analyzed (Figures S2a and S3a). In the cohort of 495 cases (60 *NOTCH1*-mut) in which CD20 expression was evaluated by the FITC-conjugated antibody, CD20 levels were generally lower in the CLL component than in the normal non-neoplastic residual B cell counterpart (Figure S2a), as reported.[27] Moreover, when CLL cases were stratified according to the classification of the main cytogenetic aberrations,[36] variable CD20 levels were found, the highest levels being detected in trisomy 12 CLL (Figure S2a).[37] When the CD20 expression was evaluated with respect to *NOTCH1* mutational status, *NOTCH1*-mut CLL expressed lower MFI values than *NOTCH1*-wt cases in both trisomy 12 CLL (mean MFI in 20 *NOTCH1*-mut cases = 1 893±196; mean MFI in 69 *NOTCH1*-wt cases = 7 051±819; $p<0.0001$) and non-trisomy 12 CLL (mean MFI in 40 *NOTCH1*-mut cases = 1 858±203; mean MFI in 366 *NOTCH1*-wt cases = 2 426±112; $p=0.017$, Figures 1a and S2b).

Superimposable results were obtained in the remaining 197 CLL (27 *NOTCH1*-mut and 170 *NOTCH1*-wt cases), in which the CD20 expression was evaluated with a PE-Cy7-conjugated antibody (Table S1), both in trisomy 12 CLL (mean MFI in 6 *NOTCH1*-mut cases = 12 926±3 676; mean MFI in 17 *NOTCH1*-wt cases = 28 216±5 228; $p=0.027$) and non-trisomy 12 CLL (mean MFI in 21 *NOTCH1*-mut cases = 10 207±1 310; mean MFI in 153 *NOTCH1*-wt cases = 15 208±1 578; $p=0.017$, Figure S3a,b).

In keeping with flow cytometry results, transcript levels of *MS4A1*, the gene encoding for CD20,[38] as evaluated in 275 cases (46 *NOTCH1*-mut), were lower in *NOTCH1*-mut than in *NOTCH1*-wt cases both in the trisomy 12 ($p=0.006$) and in the non-trisomy 12 ($p=0.019$) CLL categories (Figure 1b).

To corroborate the correlation between CD20 expression and *NOTCH1* mutations, we performed cell sorting experiments to isolate the extreme $CD20^{low}$ and $CD20^{high}$ subpopulations in five CLL cases with different *NOTCH1* mutational load (Figure S4), as determined by NGS, i.e. 3% (CLL#406), 8% (CLL#34), 27% (CLL#171), 35% (CLL#243) and 41% (CLL#266) of total DNA. As shown by NGS re-sequencing of the separated subpopulations, $CD20^{low}$ sorted cells always had a relative enrichment in the *NOTCH1* mutational burden when compared to the $CD20^{high}$ counterpart, i.e. 9% vs. 1% (CLL#406), 14% vs. 3% (CLL#34), 32% vs. 15% (CLL#171), 38% vs. 32% (CLL#243), 48% vs. 39% (CLL#266). Consistently, the amount of *MS4A1* transcripts was always significantly lower in the $CD20^{low}$ than in the $CD20^{high}$ subpopulation (Figure 1c).

NOTCH1 mutational status and susceptibility to anti-CD20 in CLL

Then we investigated if *NOTCH1* mutational status could effectively influence susceptibility to anti-CD20 immunotherapy. To evaluate the capability of rituximab to kill in-vitro CLL cells bearing or not *NOTCH1* mutations, CDC assay was performed utilizing purified CLL cells from 9 *NOTCH1*-mut and 9 *NOTCH1*-wt cases. *NOTCH1*-mut CLL cells showed significantly lower relative lysis induced by rituximab than *NOTCH1*-wt CLL cells (mean % of relative lysis = 2.5±0.8 vs. 26.3±8.9, p=0.021), and the killing capacity of rituximab directly correlated with CD20 levels (Figure 1d).

We further investigated the correlation between *NOTCH1* mutational status and susceptibility to rituximab by evaluating in three *NOTCH1*-mut cases the enrichment of *NOTCH1* mutational burden after CDC assay upon rituximab and subsequent cell sorting of the residual viable cell population. The *NOTCH1* mutational burden, as detected by NGS, resulted higher in the post-CDC sorted viable cells than in the pre-CDC unsorted counterpart in all the three tested cases (Figure 1e). Consistently, the amount of *MS4A1* transcripts, as detected by QRT-PCR, were lower in the viable cell populations than in the pre-CDC unsorted counterparts (Figure 1e).

We also evaluated the capability of the alternative anti-CD20 antibody ofatumumab to kill in-vitro CLL cells from 9 *NOTCH1*-mut and 9 *NOTCH1*-wt cases. Although the killing capacity of ofatumumab resulted generally higher than that of rituximab, *NOTCH1*-mut CLL cells showed significantly lower relative lysis than *NOTCH1*-wt CLL cells (mean % of relative lysis = 30.6±8.5 vs. 60.6±5.8, p=0.011), again consistently with CD20 expression levels (Figure 1f).

NOTCH1 signaling and CD20 expression in CLL

To evaluate if *NOTCH1* signaling could influence CD20 expression in primary CLL cases, CLL cells from 5 *NOTCH1*-mut and 6 *NOTCH1*-wt cases were treated at different time points with the GSI L-685,458, able to block the proteolytic generation of NICD.[21] Upon GSI treatment, NOTCH1 signaling was consistently impaired, as defined by a reduction of *HES1* expression (at 6 hours) in both *NOTCH1*-wt and *NOTCH1*-mut CLL, although decreases were lower in the *NOTCH1*-mut category (p=0.005), according to the presence of higher levels of NICD in the latter cases (Figure S5a and Figure S1). More important, both *MS4A1* transcripts (at 6 hours) and CD20 expression levels (at 24 hours) were significantly upregulated by GSI in *NOTCH1*-wt and, to a lesser extent, in *NOTCH1*-mut cases (Figure S5b). No effect on CD20 expression was observed in purified normal B cells from healthy donors exposed in-vitro to GSI, in keeping with the notion of a lack of NOTCH1 expression in these cells (not shown).[21]

To further confirm the association between NOTCH1 signaling and CD20 expression, CLL cells from 6 *NOTCH1*-mut and 5 *NOTCH1*-wt cases were transiently transfected with siRNA for NOTCH1. In both *NOTCH1*-mut and *NOTCH1*-wt cases, siRNA transfection effectively reduced

NOTCH1 transcript at 6 hours (p=0.001, not shown) and protein at 24 hours (*NOTCH1*-mut cases, mean MFI = 538±119 vs. 184±32, p=0.011; *NOTCH1*-wt cases, mean MFI = 524±64 vs. 204±17, p=0.003). Consistently, CD20 expression resulted augmented both at transcript level (at 6 hours, *NOTCH1*-mut, p=0.034, *NOTCH1*-wt, p= 0.012, not shown) and protein level (at 24 hours, *NOTCH1*-mut cases, mean MFI = 2685±887 vs. 3035±916, p=0.001; *NOTCH1*-wt cases, mean MFI = 1707±434 vs. 1923±434, p=0.003, Figure S5c).

Establishment of an in-vitro model of mutated NICD-transfected CLL-like cells

To investigate the mechanism(s) through which *NOTCH1* mutations may affect CD20 expression in CLL, we established an in-vitro model of NICD transfected cells by taking advantage of the CLL-like MEC-1 cell line. MEC-1 cells, constitutively expressing a wild-type *NOTCH1* form, were stably transfected with vectors encoding for: i) a modified NICD with the c.7541-7542delCT (NICD-mut); ii) a modified NICD with a nonsense mutation inserted after the beginning of the coding sequence, as a null control (NICD-null). NICD-mut cells showed higher constitutive NOTCH1 protein levels than NICD-null cells (Figure 2a). Consistently, *HES1* and *HES5* transcript levels were higher in NICD-mut than in NICD-null cells (Figure 2b).

When CD20 expression was tested, NICD-mut cells showed constitutive lower CD20 expression at both protein and transcript level than NICD-null cells (Figure 2a,c), and, consistently, lower relative lysis induced by rituximab and ofatumumab by CDC assay (p=0.043, p=0.025, respectively, Figure 2d). Moreover, upon GSI treatment, CD20 protein expression was significantly up-regulated in both NICD-null cells and NICD-mut cells (Figure 2e), as it was the transcript for the *MS4A1* gene (not shown).

According to these validations, we assumed the NICD-mut cells as in-vitro model of *NOTCH1*-mut CLL, in which the increased NICD accumulation, due to a decreased degradation of truncated form,[15] is mimicked by the enforced expression of an exogenously transfected mutated NICD.

Immunoprecipitation of the RBPJ transcription factor in NICD transfectants

When released by proteolytic cleavages and translocated into the nucleus upon activation of the NOTCH1 pathway, NICD interacts with the RBPJ transcription factor and converts its function from repressor to activator of gene transcription.[13,15,35] In fact, NICD is able to displace RBPJ from a HDAC-containing repression complex, thus forming, with RBPJ itself and other co-activators, the major gene transcriptional activation complex of the NOTCH1 pathway.[13,15,35]

To evaluate whether NICD accumulation, as it occurs upon *NOTCH1* mutations, could alter the balancing of the two functions of RBPJ, i.e. transcriptional activator (complexed with NICD) or transcriptional repressor (complexed with HDACs),[13,15] we performed co-immunoprecipitation experiments aimed at investigating the alternative presence of NICD or HDACs (namely HDAC1 and HDAC2) bound to RBPJ in NICD transfectants. As shown in Figure 3a, co-immunoprecipitation experiments revealed that NICD-mut cells had higher levels of NICD bound with RBPJ than NICD-null cells. On the contrary, NICD-mut cells showed lower levels of HDAC1 or HDAC2 co-immunoprecipitated with RBPJ than NICD-null cells (Figure 3a). Notably, no difference was found by comparing NICD transfectants regarding the levels of immunoprecipitated RBPJ, and the nuclear and cytoplasmic levels of RBPJ, HDAC1 and HDAC2, as evidenced by control WB experiments (Figure S6a,b,c). Consistently, comparable constitutive *HDAC1/HDAC2* expression levels were found in *NOTCH1*-mut versus *NOTCH1*-wt primary CLL (Figure S7).

The un-balancing of the transcriptional activation/repression equilibrium of RBPJ turned in favor of the activation of NOTCH1 signaling detected in NICD-mut cells was also in keeping with the higher *HES1* and *HES5* transcript levels detected in these cells (Figure 2b).

HDAC-mediated ChIP in NICD transfectants

Previous studies identified epigenetic silencing of CD20 expression via HDACs as a mechanism conferring resistance to rituximab in lymphomas.[34,39,40] To evaluate whether the preferential interaction of RBPJ with NICD could result in higher levels of HDAC1/HDAC2 available for the transcriptional repression of *MS4A1*,[13,15] ChIP assays were performed on nuclear lysates from NICD transfectants. As shown in Figure 3b, higher levels of DNA corresponding to the *MS4A1* promoter were found in HDAC1 and HDAC2 chromatin immunoprecipitates from NICD-mut compared to NICD-null cells. Of note, a higher involvement of HDAC2 with respect to HDAC1 was evidenced ChIP experiments, in keeping with the higher levels of HDAC2 expressed by NICD transfectants (Figure S6c). On the other hand, lower levels of DNA corresponding to the *HES1* promoter were found by ChIP of NICD-mut cells compared to NICD-null cells (not shown).

These results suggest that higher NICD levels, as occurring in NICD-mut cells, may cause a NICD-dependent dislodgement of RBPJ from the HDAC-containing repression complexes. This phenomenon is associated with an increased availability of HDACs to repress transcription of the *MS4A1* gene.

HDAC inhibition and CD20 expression

To further evaluate if the higher levels of HDACs bound to the *MS4A1* promoter could effectively affect CD20 expression, NICD transfected cells were treated with the HDAC inhibitor VPA for 48 hours. In both NICD-mut and NICD-null cells, VPA treatment was able to significantly increase *MS4A1* transcript levels (NICD-mut, mean fold increase =1.7, p=0.001; NICD-null, mean fold increase =1.5 p=0.003, Figure S8a) and CD20 protein expression (NICD-mut, mean fold increase =1.3, p=0.041; NICD-null, mean fold increase =1.4, p=0.029, Figure 4a,b).

Similar results were obtained by treating with VPA primary CLL cells of 7 *NOTCH1*-mut and 6 *NOTCH1*-wt cases. In both categories, VPA treatment was able to significantly increase *MS4A1* transcripts (*NOTCH1*-mut, mean fold increase =1.5, p=0.05; *NOTCH1*-wt, mean fold increase = 1.8, p=0.02, Figure S8b) and CD20 protein (*NOTCH1*-mut, mean fold increase = 1.3, p=0.05; *NOTCH1*-wt, mean fold increase = 1.3, p=0.005, Figure 4c,d). These increments were not associated with significant increases of relative lysis by in-vitro CDC assays (not shown).

Discussion

The FCR immuno-chemotherapy combination still represents the frontline regimen for treatment of patients in good physical conditions.[1,2] In particular, the addition of rituximab to the FC combination has been definitely proved to improve the clinical outcome of CLL patients, despite the relative low levels of CD20 usually expressed on the surface of CLL cells.[26,27] Recently, however, it has been clearly demonstrated that such a benefit does not include patients affected by CLL bearing *NOTCH1* mutations,[26,41] although the reason for this different clinical behaviour remains to be elucidated.

In the present study, we demonstrated that *NOTCH1* mutations identify a CLL subset characterized by particularly low levels of CD20, both in non-trisomy 12 CLL, and in the trisomy 12 CLL category, that usually has relatively higher CD20 levels and a higher frequency of *NOTCH1* mutations.[9,10,37] Conversely, Stilgenbauer *et al* did not find any difference in CD20 expression between *NOTCH1*-mut and *NOTCH1*-wt CLL although in this study CD20 levels were checked exclusively by flow cytometry in a minority of cases.[26] Here, the lower CD20 expression by *NOTCH1*-mut cases was corroborated by the parallel finding of lower *MS4A1* transcript levels. Moreover, in cell sorting experiments of CLL cases with different *NOTCH1* mutation levels, higher percentages of *NOTCH1* mutated DNA were found in the sorted $CD20^{low}$ component compared to the $CD20^{high}$ counterpart. Finally, the dramatic downregulation of CD20 expression levels obtained by stably transfecting the CLL-like MEC-1 cells with a mutated NICD definitely confirmed this inverse correlation.

The low CD20 expression by *NOTCH1*-mut CLL cells is consistent with their lower sensitivity to rituximab and ofatumumab exposure in-vitro, as shown here, in agreement with previous reports.[42] Results of the present study also indicate that the residual CLL cells surviving upon CDC assay with rituximab, usually expressed lower CD20 levels and a greater *NOTCH1* mutational load. In keeping, *NOTCH1* mutations have been demonstrated to impact on rituximab sensitivity of CLL patients also when present at subclonal level.[26,41,43]

These data may also suggest that, in CLL, the constitutive expression of NOTCH1, in its mutated configuration but also in the wild type form,[21] could be related with the generally lower CD20 levels observed in neoplastic versus normal B cells, in which NOTCH1 is not expressed at all.[21] In keeping, we demonstrated here that GSI treatment in-vitro was able to substantially augment CD20 expression both in *NOTCH1*-wt and *NOTCH1*-mut CLL cells, although in the latter the accumulation of NICD due to truncating mutations makes these cells relatively less susceptible to NOTCH1 signaling perturbation. Since theoretically GSI may have off-target genes,[44] NOTCH1 was also inhibited by specific siRNA. Again, transfection with siRNA increased CD20 expression both in *NOTCH1*-wt and *NOTCH1*-mut CLL cells.[35]

In humans, the balance of hystone acetylation/deacetylation, respectively induced by hystone acetyl transferases and HDACs, represents one of the main epigenetic mechanisms of modification of chromatin conformation and regulation of gene expression.[45,46] In particular, the transcriptional activity due to the triggering of the NOTCH1 pathway is known to be greatly sensitive to chromatin modifications and hystone rearrangements.[35] In this context, the main effector of the NOTCH1 pathway at nuclear level is a DNA-binding protein named RBPJ.[13,15,35] This protein, in association with NICD and other co-activators forms an activation complex that is essential for NICD-dependent transcription and target gene expression. Such an activation complex is degraded via NICD phosphorylation, and its subsequent ubiquitination, these molecular reactions requiring an

intact C-terminal PEST region of the NICD protein.[13,15,35] The specific degradation of NICD results in the dissociation among RBPJ and the other co-activators. In the absence of NICD, RBPJ is free to associate with specific co-repressors, which in turn recruit HDAC1 and HDAC2; this newly obtained repression complex represses NOTCH1 signaling.[13,15,35]. A simplified scheme of these multi-protein interactions is reported in Figure 5a.

Results of this study suggest that NOTCH1 with C-terminal truncations, as those determined by the c.7541-7542delCT, may influence the epigenetic downregulation of CD20 by HDACs allegedly via an impaired ubiquitination and degradation of the truncated NICD. In fact, as defined by co-immunoprecipitation experiments, in the condition of NICD accumulation due to the c.7541-7542delCT, RBPJ showed a preferential binding to NICD, in the context of the activation complex, rather than to HDACs, in the context of the repression complex. In NICD-mut cells, in turn, HDACs were mainly associated to the *MS4A1* promoter, as defined by ChIP experiments. A necessary prerequisite is the persistence of the activation complex due to the lack of degradation of the truncated NICD (Figure 5b).[13,15,35] In keeping, the rare *NOTCH1*-mut CLL carrying truncating mutations other than the c.7541-7542delCT (6 cases in our cohort) were all characterized by low CD20 levels, comparable with those of *NOTCH1*-mut CLL carrying the c.7541-7542delCT. Conversely, three cases (not included in this cohort) carrying *NOTCH1* missense mutations (e.g. p.G2292R, p.V2214M and p.T2484M) expressed CD20 levels comparable with those of *NOTCH1*-wt CLL (F.P., personal communication).

To restore epigenetic regulation, a wide range of compounds inhibiting HDAC functionality have been identified, some of them employed in anticancer therapies.[45,46] In addition, HDAC inhibitors are known to augment the cytotoxic activity of rituximab by increasing CD20 expression in lymphoma cells.[34,39,40] In this study, treatment with the HDAC inhibitor VPA was capable to up-regulate both *MS4A1* transcript and CD20 protein either in NICD transfected cells or in primary CLL cells from *NOTCH1*-mut and *NOTCH1*-wt cases.

In conclusion, we provided evidence that truncating *NOTCH1* mutations in CLL are associated with low CD20 expression, and with a relative resistance to anti-CD20 immunotherapy in-vitro. The low CD20 expression in *NOTCH1*- mut CLL can be ascribed to a *NOTCH1* mutation-driven epigenetic dysregulation of a transcriptional repression mechanism involving HDACs. Clinically, drugs interfering with the NOTCH1 pathway and/or inhibiting HDACs might have a role to increase CD20 expression in-vivo, thus overcoming the relative resistance of *NOTCH1*-mut CLL to rituximab-containing therapies.

Acknowledgements

Supported in part by: the Associazione Italiana Ricerca Cancro (AIRC), Investigator Grant IG-13227; Progetto Ricerca Finalizzata I.R.C.C.S. n. RF-2009-1469205, n. RF-2010-2307262, Progetto Giovani Ricercatori n. GR-2009-1475467, n. GR-2010-2317594, n. GR-2011-02347441, n. GR-2011-02346826, Ministero della Salute, Rome, Italy; Fondazione Cariplo (grant 2012-0689); Associazione Italiana contro le Leucemie, linfomi e mielomi (AIL), Venezia Section, Pramaggiore Group, Italy; Fondazione per la Vita di Pordenone, Italy; Ricerca Scientifica Applicata, Regione Friuli Venezia Giulia ("Linfonet" Project), Trieste, Italy; "5x1000 Intramural Program", Centro di Riferimento Oncologico, Aviano, Italy. FA is supported by a Beat-Leukemia fellowship.

Authorship Contributions

F.P. contributed to write the manuscript, analyzed the data and performed the research, T.B. performed the research, F.A., P.B., P.M., E.T., B.G., F.M.R., R.B., A.Z., D.B., M.D., contributed to perform the research, G.D.A., A.C., F.Z., G.P., D.R., G.G., G.D.P., S.D. provided well characterized biological samples and contributed to write the manuscript, V.G. and M.D.B. designed the study, interpreted data, and wrote the manuscript.

Conflict of Interest

The Authors declare no competing financial interests.

Supplementary information is available at Leukemia's website.

References

1 Hallek M, Cheson BD, Catovsky D, Caligaris-Cappio F, Dighiero G, Dohner H *et al*. Guidelines for the diagnosis and treatment of chronic lymphocytic leukemia: a report from the International Workshop on Chronic Lymphocytic Leukemia updating the National Cancer Institute-Working Group 1996 guidelines. *Blood* 2008; **111**: 5446-5456.

2 Hallek M. Chronic lymphocytic leukemia: 2013 update on diagnosis, risk stratification and treatment. *Am J Hematol* 2013; **88**: 803-816.

3 Fabbri G, Rasi S, Rossi D, Trifonov V, Khiabanian H, Ma J *et al*. Analysis of the chronic lymphocytic leukemia coding genome: role of NOTCH1 mutational activation. *J Exp Med* 2011; **208**: 1389-1401.

4 Puente XS, Pinyol M, Quesada V, Conde L, Ordonez GR, Villamor N *et al*. Whole-genome sequencing identifies recurrent mutations in chronic lymphocytic leukaemia. *Nature* 2011; **475**: 101-105.

5 Rossi D, Rasi S, Spina V, Bruscaggin A, Monti S, Ciardullo C *et al*. Integrated mutational and cytogenetic analysis identifies new prognostic subgroups in chronic lymphocytic leukemia. *Blood* 2013; **121**: 1403-1412.

6 Quesada V, Conde L, Villamor N, Ordonez GR, Jares P, Bassaganyas L *et al*. Exome sequencing identifies recurrent mutations of the splicing factor SF3B1 gene in chronic lymphocytic leukemia. *Nat Genet* 2012; **44**: 47-52.

7 Wang L, Lawrence MS, Wan Y, Stojanov P, Sougnez C, Stevenson K *et al*. SF3B1 and other novel cancer genes in chronic lymphocytic leukemia. *N Engl J Med* 2011; **365**: 2497-2506.

8 Del Poeta G, Dal Bo M, Del Principe MI, Pozzo F, Rossi FM, Zucchetto A *et al*. Clinical significance of c.7544-7545 delCT NOTCH1 mutation in chronic lymphocytic leukaemia. *Br J Haematol* 2013; **160**: 415-418.

9 Del Giudice I, Rossi D, Chiaretti S, Marinelli M, Tavolaro S, Gabrielli S *et al*. NOTCH1 mutations in +12 chronic lymphocytic leukemia (CLL) confer an unfavorable prognosis, induce a distinctive transcriptional profiling and refine the intermediate prognosis of +12 CLL. *Haematologica* 2012; **97**: 437-441.

10 Rossi D, Rasi S, Fabbri G, Spina V, Fangazio M, Forconi F *et al*. Mutations of NOTCH1 are an independent predictor of survival in chronic lymphocytic leukemia. *Blood* 2012; **119**: 521-529.

11 Lobry C, Oh P, Aifantis I. Oncogenic and tumor suppressor functions of Notch in cancer: it's NOTCH what you think. *J Exp Med* 2011; **208**: 1931-1935.

12 Yuan JS, Kousis PC, Suliman S, Visan I, Guidos CJ. Functions of notch signaling in the immune system: consensus and controversies. *Annu Rev Immunol* 2010; **28**: 343-365.

13 Castel D, Mourikis P, Bartels SJ, Brinkman AB, Tajbakhsh S, Stunnenberg HG. Dynamic binding of RBPJ is determined by Notch signaling status. *Genes Dev* 2013; **27**: 1059-1071.

14 Davis RL, Turner DL. Vertebrate hairy and Enhancer of split related proteins: transcriptional repressors regulating cellular differentiation and embryonic patterning. *Oncogene* 2001; **20**: 8342-8357.

15 Hsieh JJ, Hayward SD. Masking of the CBF1/RBPJ kappa transcriptional repression domain by Epstein-Barr virus EBNA2. *Science* 1995; **268**: 560-563.

16 Iso T, Kedes L, Hamamori Y. HES and HERP families: multiple effectors of the Notch signaling pathway. *J Cell Physiol* 2003; **194**: 237-255.

17 Jarriault S, Brou C, Logeat F, Schroeter EH, Kopan R, Israel A. Signalling downstream of activated mammalian Notch. *Nature* 1995; **377**: 355-358.

18 Kato H, Taniguchi Y, Kurooka H, Minoguchi S, Sakai T, Nomura-Okazaki S *et al*. Involvement of RBP-J in biological functions of mouse Notch1 and its derivatives. *Development* 1997; **124**: 4133-4141.

19 Klinakis A, Szabolcs M, Politi K, Kiaris H, rtavanis-Tsakonas S, Efstratiadis A. Myc is a Notch1 transcriptional target and a requisite for Notch1-induced mammary tumorigenesis in mice. *Proc Natl Acad Sci U S A* 2006; **103**: 9262-9267.

20 Weng AP, Millholland JM, Yashiro-Ohtani Y, Arcangeli ML, Lau A, Wai C *et al*. c-Myc is an important direct target of Notch1 in T-cell acute lymphoblastic leukemia/lymphoma. *Genes Dev* 2006; **20**: 2096-2109.

21 Rosati E, Sabatini R, Rampino G, Tabilio A, Di IM, Fettucciari K *et al*. Constitutively activated Notch signaling is involved in survival and apoptosis resistance of B-CLL cells. *Blood* 2009; **113**: 856-865.

22 Paganin M, Ferrando A. Molecular pathogenesis and targeted therapies for NOTCH1-induced T-cell acute lymphoblastic leukemia. *Blood Rev* 2011; **25**: 83-90.

23 Weng AP, Ferrando AA, Lee W, Morris JP, Silverman LB, Sanchez-Irizarry C *et al*. Activating mutations of NOTCH1 in human T cell acute lymphoblastic leukemia. *Science* 2004; **306**: 269-271.

24 Sportoletti P, Baldoni S, Cavalli L, Del PB, Bonifacio E, Ciurnelli R *et al*. NOTCH1 PEST domain mutation is an adverse prognostic factor in B-CLL. *Br J Haematol* 2010; **151**: 404-406.

25 Arruga F, Gizdic B, Serra S, Vaisitti T, Ciardullo C, Coscia M *et al*. Functional impact of NOTCH1 mutations in chronic lymphocytic leukemia. *Leukemia* 2014; **28**: 1060-1070.

26 Stilgenbauer S, Schnaiter A, Paschka P, Zenz T, Rossi M, Dohner K *et al*. Gene mutations and treatment outcome in chronic lymphocytic leukemia: results from the CLL8 trial. *Blood* 2014; **123**: 3247-3254.

27 Matutes E, Owusu-Ankomah K, Morilla R, Garcia MJ, Houlihan A, Que TH *et al*. The immunological profile of B-cell disorders and proposal of a scoring system for the diagnosis of CLL. *Leukemia* 1994; **8**: 1640-1645.

28 Gattei V, Bulian P, Del Principe MI, Zucchetto A, Maurillo L, Buccisano F *et al*. Relevance of CD49d protein expression as overall survival and progressive disease prognosticator in chronic lymphocytic leukemia. *Blood* 2008; **111**: 865-873.

29 Zucchetto A, Vaisitti T, Benedetti D, Tissino E, Bertagnolo V, Rossi D *et al*. The CD49d/CD29 complex is physically and functionally associated with CD38 in B-cell chronic lymphocytic leukemia cells. *Leukemia* 2012; **26**: 1301-1312.

30 Rossi D, Spina V, Bomben R, Rasi S, Dal-Bo M, Bruscaggin A *et al*. Association between molecular lesions and specific B-cell receptor subsets in chronic lymphocytic leukemia. *Blood* 2013; **121**: 4902-4905.

31 Balatti V, Bottoni A, Palamarchuk A, Alder H, Rassenti LZ, Kipps TJ *et al*. NOTCH1 mutations in CLL associated with trisomy 12. *Blood* 2012; **119**: 329-331.

32 Bomben R, Gobessi S, Dal BM, Volinia S, Marconi D, Tissino E *et al*. The miR-17 approximately 92 family regulates the response to Toll-like receptor 9 triggering of CLL cells with unmutated IGHV genes. *Leukemia* 2012; **26**: 1584-1593.

33 Saborit-Villarroya I, Vaisitti T, Rossi D, D'Arena G, Gaidano G, Malavasi F *et al*. E2A is a transcriptional regulator of CD38 expression in chronic lymphocytic leukemia. *Leukemia* 2011; **25**: 479-488.

34 Sugimoto T, Tomita A, Hiraga J, Shimada K, Kiyoi H, Kinoshita T *et al*. Escape mechanisms from antibody therapy to lymphoma cells: downregulation of CD20 mRNA by recruitment of the HDAC complex and not by DNA methylation. *Biochem Biophys Res Commun* 2009; **390**: 48-53.

35 Bray SJ. Notch signalling: a simple pathway becomes complex. *Nat Rev Mol Cell Biol* 2006; **7**: 678-689.

36 Dohner H, Stilgenbauer S, Benner A, Leupolt E, Krober A, Bullinger L *et al*. Genomic aberrations and survival in chronic lymphocytic leukemia. *N Engl J Med* 2000; **343**: 1910-1916.

37 Tam CS, Otero-Palacios J, Abruzzo LV, Jorgensen JL, Ferrajoli A, Wierda WG *et al*. Chronic lymphocytic leukaemia CD20 expression is dependent on the genetic subtype: a study of quantitative flow cytometry and fluorescent in-situ hybridization in 510 patients. *Br J Haematol* 2008; **141**: 36-40.

38 Tedder TF, Streuli M, Schlossman SF, Saito H. Isolation and structure of a cDNA encoding the B1 (CD20) cell-surface antigen of human B lymphocytes. *Proc Natl Acad Sci U S A* 1988; **85**: 208-212.

39 Hiraga J, Tomita A, Sugimoto T, Shimada K, Ito M, Nakamura S *et al*. Down-regulation of CD20 expression in B-cell lymphoma cells after treatment with rituximab-containing combination chemotherapies: its prevalence and clinical significance. *Blood* 2009; **113**: 4885-4893.

40 Shimizu R, Kikuchi J, Wada T, Ozawa K, Kano Y, Furukawa Y. HDAC inhibitors augment cytotoxic activity of rituximab by upregulating CD20 expression on lymphoma cells. *Leukemia* 2010; **24**: 1760-1768.

41 Bo MD, Del Principe MI, Pozzo F, Ragusa D, Bulian P, Rossi D *et al*. NOTCH1 mutations identify a chronic lymphocytic leukemia patient subset with worse prognosis in the setting of a rituximab-based induction and consolidation treatment. *Ann Hematol* 2014; **93**: 1765-1774.

42 Golay J, Lazzari M, Facchinetti V, Bernasconi S, Borleri G, Barbui T *et al*. CD20 levels determine the in vitro susceptibility to rituximab and complement of B-cell chronic lymphocytic leukemia: further regulation by CD55 and CD59. *Blood* 2001; **98**: 3383-3389.

43 Sportoletti P, Baldoni S, Del PB, Aureli P, Dorillo E, Ruggeri L *et al*. A revised NOTCH1 mutation frequency still impacts survival while the allele burden predicts early progression in chronic lymphocytic leukemia. *Leukemia* 2014; **28**: 436-439.

44 Andersson ER, Lendahl U. Therapeutic modulation of Notch signalling--are we there yet? *Nat Rev Drug Discov* 2014; **13**: 357-378.

45 Minucci S, Pelicci PG. Histone deacetylase inhibitors and the promise of epigenetic (and more) treatments for cancer. *Nat Rev Cancer* 2006; **6**: 38-51.

46 Ropero S, Esteller M. The role of histone deacetylases (HDACs) in human cancer. *Mol Oncol* 2007; **1**: 19-25.

Figure legends

Figure 1. Correlation between *NOTCH1* mutations, CD20 expression, and susceptibility to anti-CD20 antibodies in CLL (a) Box-and-whiskers plots showing CD20 protein expression levels, evaluated as above, in 89 trisomy 12 CLL cases (20 *NOTCH1*-mut cases, 69 *NOTCH1*-wt cases) and 406 non-trisomy 12 CLL cases (40 *NOTCH1*-mut cases, 366 *NOTCH1*-wt cases). The corresponding p values are reported. **(b)** Box-and-whiskers plots showing *MS4A1* transcript expression levels, as evaluated by QRT-PCR, in 52 trisomy 12 CLL cases (15 *NOTCH1*-mut cases, 37 *NOTCH1*-wt cases) and 223 non-trisomy 12 CLL cases (31 *NOTCH1*-mut cases, 192 *NOTCH1*-wt cases). The corresponding p values are reported. **(c)** Histograms showing *NOTCH1* mutational load (upper panel), as determined by NGS and expressed in percentage of *NOTCH1*-mut DNA, and *MS4A1* transcript levels, as determined by QRT-PCR, in the $CD20^{low}$ and $CD20^{high}$ subpopulations, as obtained by performing a cell sorting in 5 *NOTCH1*-mut CLL cases. **(d)** Box-and-whiskers plots showing the percentage of relative lysis of CLL cells, from *NOTCH1*-mut and *NOTCH1*-wt CLL cases, treated with rituximab in a standard CDC assay. The corresponding p value is reported (left panel). Correlation graph showing CD20 expression versus percentage of relative lysis in *NOTCH1*-mut and *NOTCH1*-wt CLL cases, as evaluated by CDC assay (r= Pearson correlation coefficient, right panel). **(e)** Histograms showing *NOTCH1* mutational load (upper panel), as determined by NGS and expressed in percentage of *NOTCH1*-mut DNA, and *MS4A1* transcript levels, as determined by QRT-PCR, in the viable cell subpopulation after CDC (post-CDC) with rituximab, and in the pre-CDC unsorted counterpart (pre-CDC), by performing a cell sorting in 3 *NOTCH1*-mut CLL cases. **(f)** Box-and-whiskers plots showing the percentage of relative lysis of CLL cells, from *NOTCH1*-mut and *NOTCH1*-wt CLL cases, treated with ofatumumab in a standard CDC assay. The corresponding p value is reported (left panel). Correlation graph showing CD20 expression versus percentage of relative lysis in *NOTCH1*-mut and *NOTCH1*-wt CLL cases, as evaluated by CDC assay (r= Pearson correlation coefficient, right panel).

Figure 2. Establishment of an in-vitro model of mutated NICD-transfected CLL-like cells. (a) NOTCH1 and CD20 protein expression levels of NICD-null and NICD-mut cells, as evaluated by WB. β-actin was used as loading control. Exogenous transfected mutated NICD is indicated as GFP-NICD, endogenous NICD is indicated as NICD. **(b)** Histograms showing constitutive *HES1* and *HES5* expression levels of NICD-null and NICD-mut cells, as evaluated by QRT-PCR. The corresponding p values are reported. **(c)** Histograms (left panel) and box-and-whiskers plots (middle panel) showing constitutive *MS4A1* transcript and CD20 protein expression levels of NICD-null and NICD-mut cells, as evaluated by QRT-PCR and flow cytometry, respectively. The corresponding p values are reported. Right panel reports a representative overlay histogram of CD20 expression in NICD-null (empty histogram) and NICD-mut (grey histogram). **(d)** Box-and-whiskers plots showing the percentage of relative lysis of NICD-null (empty histogram) and NICD-mut cells (grey histogram), upon rituximab or ofatumumab, as evaluated by CDC assay. The corresponding p value are reported. Results of three independent experiments are reported. **(e)** Box-and-whiskers plots showing CD20 protein expression levels of NICD-null and NICD-mut cells, untreated (UNT) and upon GSI treatment (GSI) for 24 hours, as evaluated by flow cytometry. The corresponding p values are reported. Results of three independent experiments are reported.

Figure 3. Characterization of a HDAC dependent epigenetic repression mechanism of CD20 expression in NICD transfected cells. (a) Immunoblotting with antibodies recognizing the total NOTCH1 (upper panel), HDAC1 (middle panel), and HDAC2 (lower panel) in whole nuclear lysates (WNL), immunoprecipitates with isotypic control (ISO) and immunoprecipitated with RBPJ (RBPJ) derived from NICD-mut and NICD-null cells. Exogenous transfected mutated NICD is

indicated as GFP-NICD, endogenous NICD is indicated as NICD. **(b)** Analysis of the *MS4A1* promoter in total chromatin preparation (INPUT), and ChIP with isotypic control (ISO), antibodies recognizing HDAC1 and HDAC2, as evaluated by qualitative PCR (upper panel). Results from a representative experiment out of three experiments is reported. Analysis of the *MS4A1* promoter in ChIP with isotypic control (ISO), antibodies recognizing HDAC1 and HDAC2, as evaluated by QRT-PCR (lower panel). Results of three independent experiments are reported.

Figure 4. Induction of CD20 expression by HDAC inhibition in NICD transfectants and in primary CLL cells. (a) Box-and-whiskers plots showing CD20 protein expression levels of NICD-mut and NICD-null cells, untreated (UNT) and VPA treated (VPA) for 48 hours, as evaluated by flow cytometry. The corresponding p values are reported. Results of three independent experiments are showed. **(b)** Representative overlay histograms showing CD20 expression levels of NICD-mut and NICD-null cells, untreated (UNT) and VPA treated (VPA) for 48 hours, as evaluated by flow cytometry. **(c)** Dot-and-line diagrams showing CD20 expression levels in primary CLL cells, untreated (UNT) and VPA treated (VPA) for 48 hours, from *NOTCH1*-mut and *NOTCH1*-wt cases, as evaluated by flow cytometry. The corresponding p values are reported. **(d)** Representative overlay histograms showing CD20 expression levels of CLL cell samples, untreated and VPA treated for 48 hours, of prototypic *NOTCH1*-mut and *NOTCH1*-wt cases, as evaluated by flow cytometry.

Figure 5. Putative model of a *NOTCH1* mutation-dependent mechanism of CD20 down-regulation via HDAC1/HDAC2 epigenetic repression in CLL. (a) Regulated balancing in *NOTCH1*-wt CLL (phospho, phosphorylation; ub, ubiquitination; Co-A, co-activators; Co-R, co-repressors). **(b)** Dysregulated balancing in *NOTCH1*-mut CLL. See text for further details.

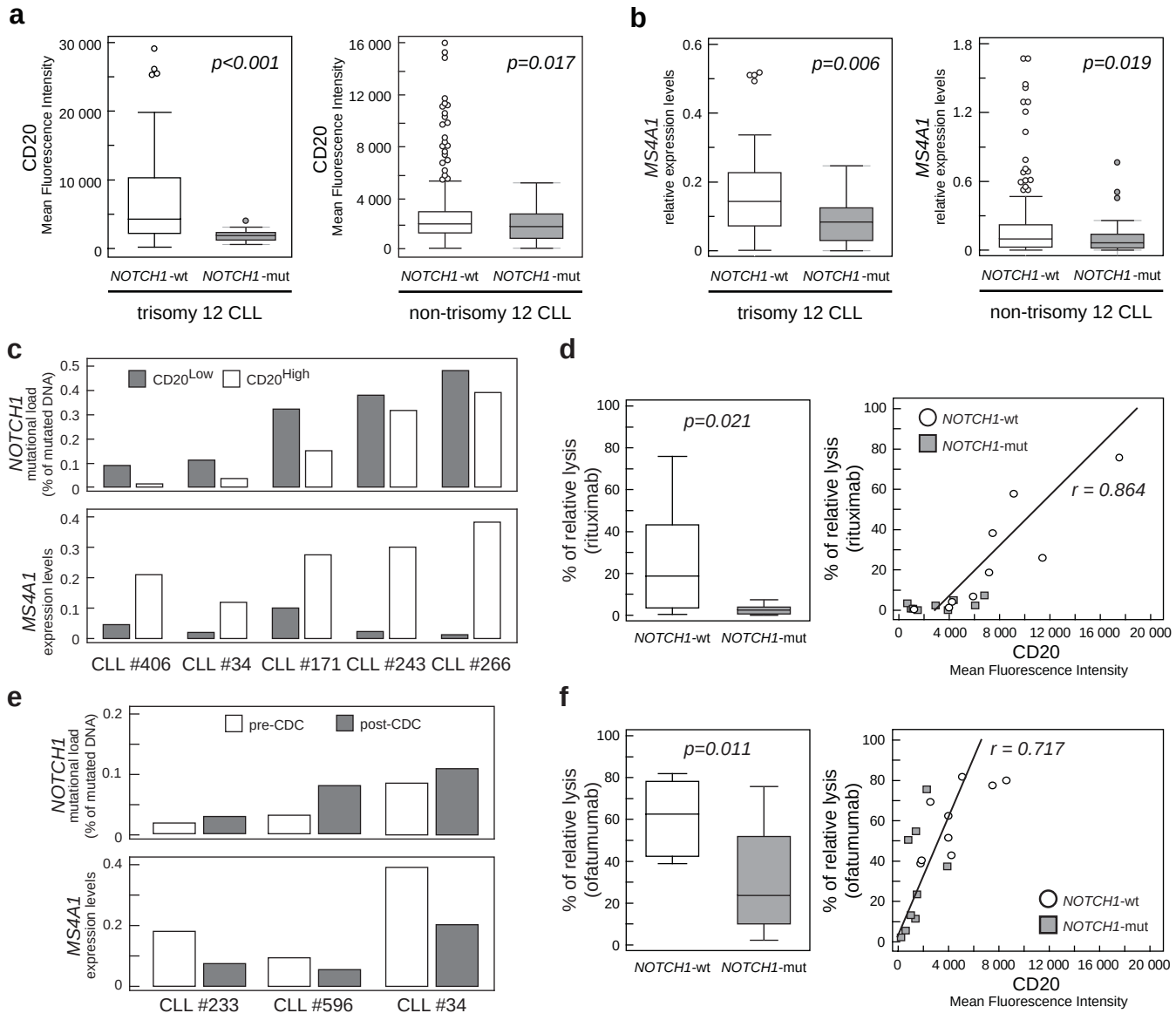
a
CD20
Mean Fluorescence Intensity
p<0.001
NOTCH1-wt
NOTCH1-mut
trisomy 12 CLL
p=0.017
non-trisomy 12 CLL
b
MS4A1
relative expression levels
p=0.006
p=0.019
c
NOTCH1
mutational load
(% of mutated DNA)
CD20Low
CD20High
MS4A1
expression levels
CLL #406
CLL #34
CLL #171
CLL #243
CLL #266
d
% of relative lysis
(rituximab)
p=0.021
r = 0.864
e
pre-CDC
post-CDC
CLL #233
CLL #596
CLL #34
f
(ofatumumab)
p=0.011
r = 0.717

Figure 1

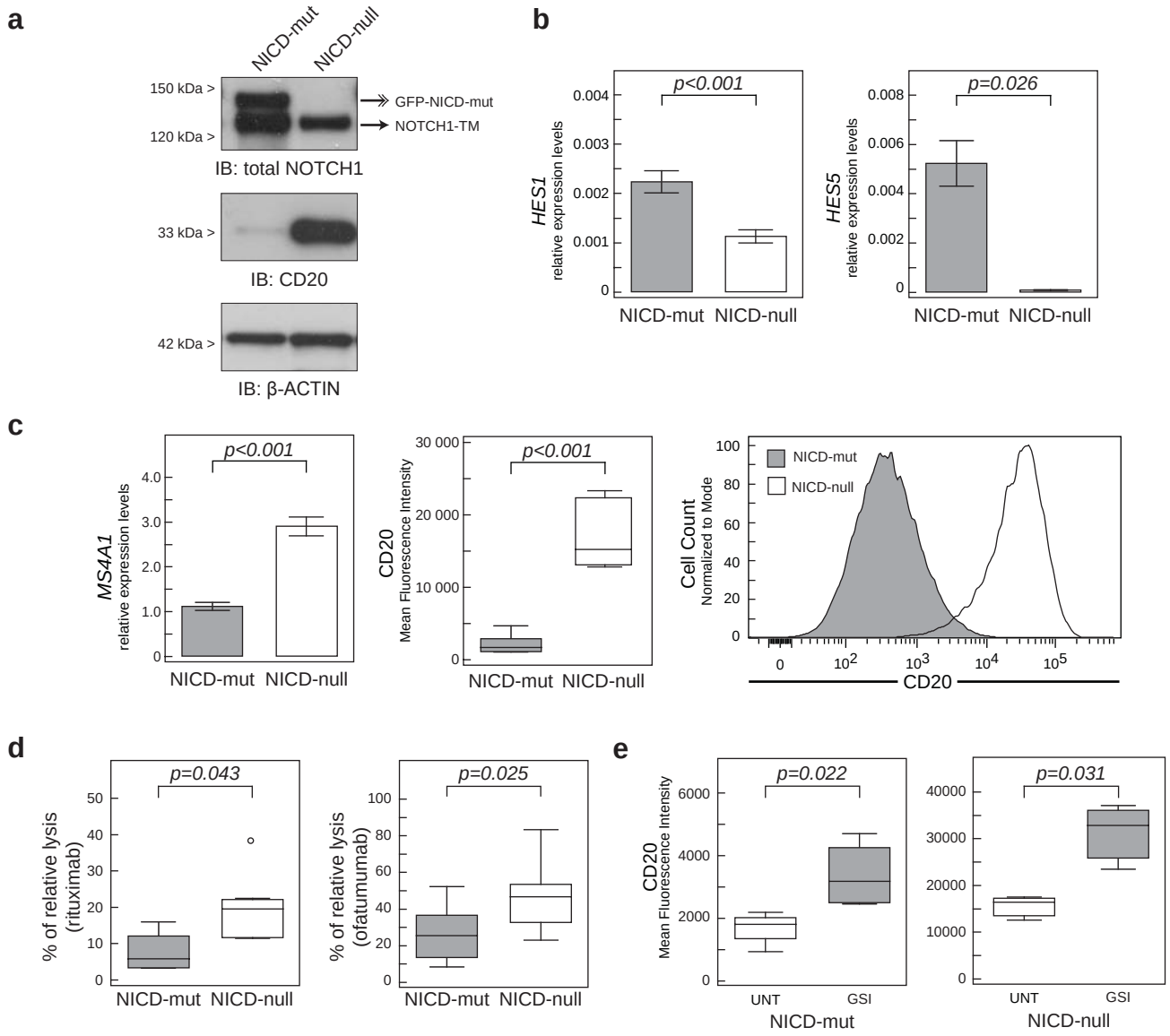
a
NICD-mut
NICD-null
150 kDa >
120 kDa >
GFP-NICD-mut
NOTCH1-TM
IB: total NOTCH1
33 kDa >
IB: CD20
42 kDa >
IB: β-ACTIN
b
HES1
relative expression levels
p<0.001
NICD-mut NICD-null
HES5
relative expression levels
p=0.026
NICD-mut NICD-null
c
MS4A1
relative expression levels
p<0.001
NICD-mut NICD-null
CD20
Mean Fluorescence Intensity
p<0.001
NICD-mut NICD-null
Cell Count
Normalized to Mode
NICD-mut
NICD-null
CD20
d
% of relative lysis (rituximab)
p=0.043
NICD-mut NICD-null
% of relative lysis (ofatumumab)
p=0.025
NICD-mut NICD-null
e
CD20
Mean Fluorescence Intensity
p=0.022
UNT GSI
NICD-mut
p=0.031
UNT GSI
NICD-null

Figure 2

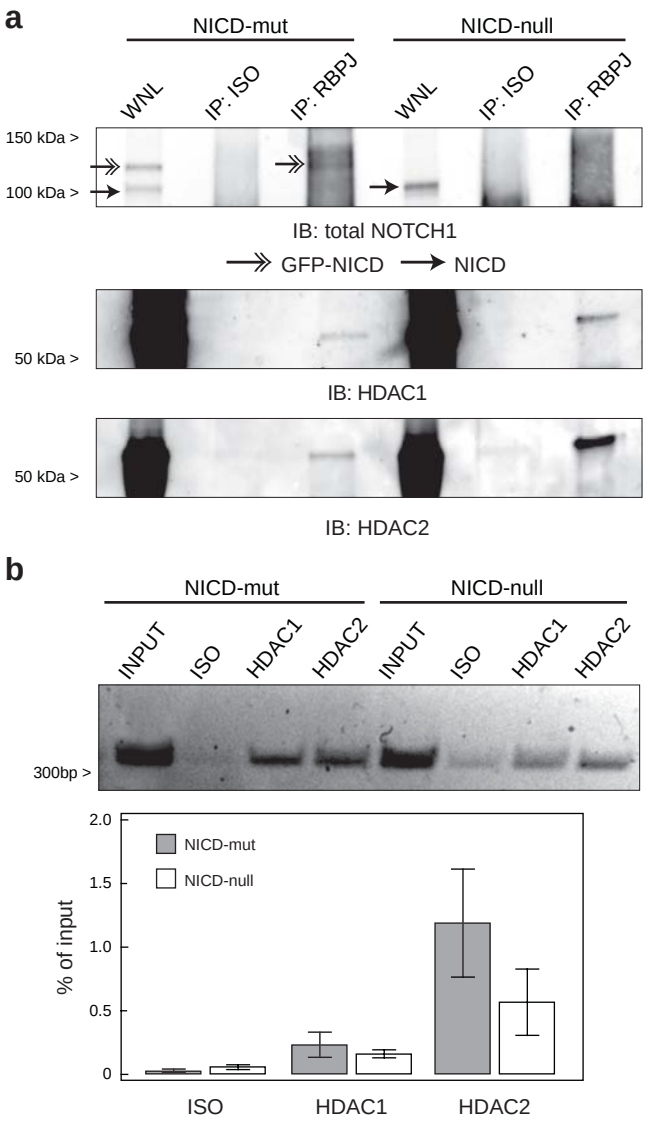
a
NICD-mut
NICD-null
WNL
IP: ISO
IP: RBPJ
WNL
IP: ISO
IP: RBPJ
150 kDa >
100 kDa >
IB: total NOTCH1
GFP-NICD
NICD
50 kDa >
IB: HDAC1
50 kDa >
IB: HDAC2
b
NICD-mut
NICD-null
INPUT
ISO
HDAC1
HDAC2
INPUT
ISO
HDAC1
HDAC2
300bp >
2.0
1.5
1.0
0.5
0
% of input
NICD-mut
NICD-null
ISO
HDAC1
HDAC2

Figure 3

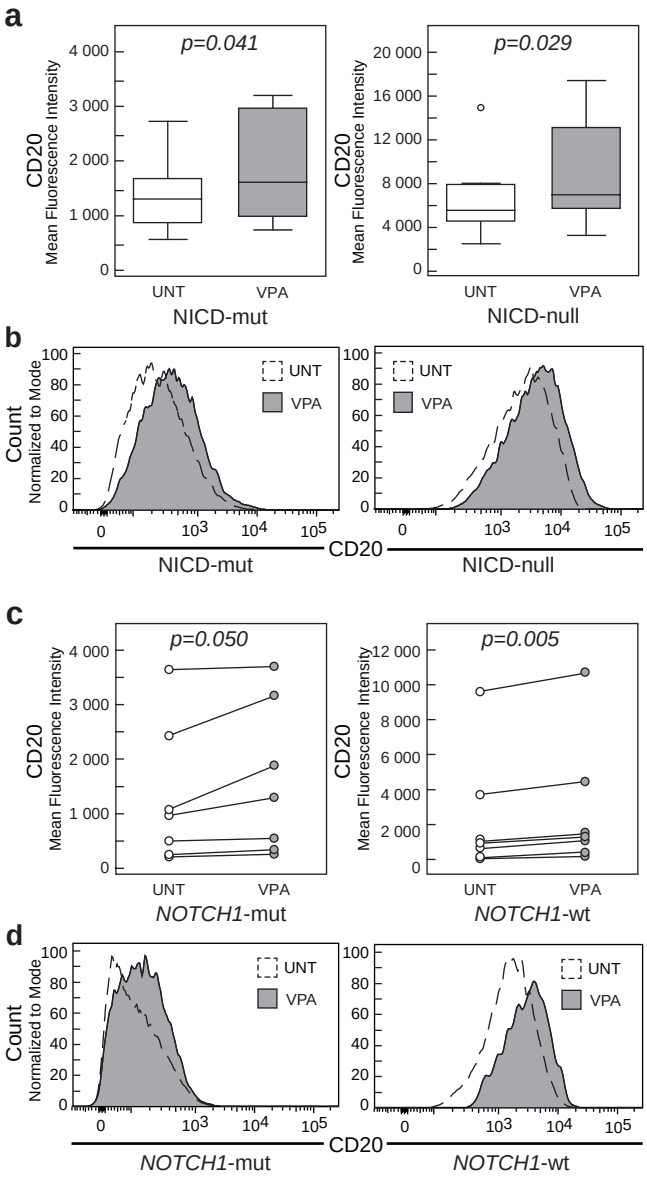
a
p=0.041
p=0.029
CD20
Mean Fluorescence Intensity
UNT
VPA
NICD-mut
NICD-null
b
Count
Normalized to Mode
UNT
VPA
CD20
NICD-mut
NICD-null
c
p=0.050
p=0.005
NOTCH1-mut
NOTCH1-wt
d
NOTCH1-mut
NOTCH1-wt

Figure 4

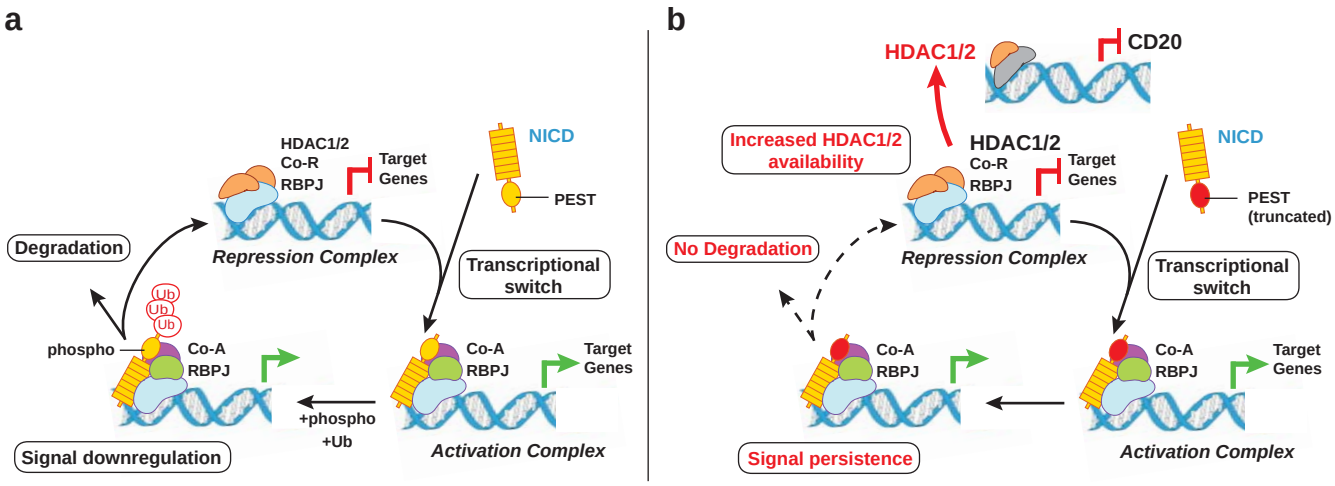
a
HDAC1/2
Co-R
RBPJ
Target
Genes
NICD
PEST
Degradation
Repression Complex
Transcriptional
switch
Ub
Ub
Ub
phospho
Co-A
RBPJ
Co-A
RBPJ
Target
Genes
+phospho
+Ub
Signal downregulation
Activation Complex
b
HDAC1/2
CD20
Increased HDAC1/2
availability
HDAC1/2
Co-R
RBPJ
Target
Genes
NICD
PEST
(truncated)
No Degradation
Repression Complex
Transcriptional
switch
Co-A
RBPJ
Co-A
RBPJ
Target
Genes
Signal persistence
Activation Complex

Figure 5

NOTCH1 mutations associate with low CD20 level in chronic lymphocytic leukemia: evidence for a *NOTCH1* mutation-driven epigenetic dysregulation

Supplementary information:

- **Supplementary Materials and Methods**
- **Supplementary Tables:**
  - Table S1. Biological characterization of the CLL cohort (692 cases).
  - Table S2. *NOTCH1* mutation features of the *NOTCH1* mutated cohort (87 cases).
- **Supplementary Figure Legends**
- **Supplementary Figures**
  - Figure S1. NOTCH1 transmembrane and NICD protein expression in *NOTCH1*-mut and *NOTCH1*-wt CLL cases.
  - Figure S2. CD20 expression levels in CLL cells (first series) and in normal B cells from healthy donors.
  - Figure S3. CD20 expression levels in CLL cells (second series), divided according to cytogenetic abnormalities.
  - Figure S4. Cell sorting of $CD20^{low}$ and $CD20^{high}$ subpopulations in *NOTCH1*-mut CLL cases.
  - Figure S5. Induction of CD20 expression by NOTCH1 signaling inhibition in *NOTCH1*-mut and *NOTCH1*-wt CLL cases.
  - Figure S6. Loading controls for the RBPJ co-immunoprecipation.
  - Figure S7. Constitutive *HDAC1* and *HDAC2* expression levels in *NOTCH1*-mut and *NOTCH1*-wt CLL cases.
  - Figure S8. Induction of *MS4A1* transcript expression by HDAC inhibition in-vitro.

Supplementary Materials and Methods

CD20 expression

For CD20 expression analyses, these two cohorts were kept separated. CD20 expression was evaluated in the neoplastic (i.e. $CD19^+$, $CD5^+$, κ/λ clonal) and residual normal B cell (i.e. $CD19^+$ $CD5^-$) components. CD20 expression after in-vitro experiments was evaluated using a PE-conjugated anti-CD20 antibody (clone L27, BD Biosciences). CD20 levels were expressed as Mean Fluorescence Intensity (MFI) in $\log_{10}$ mode. Irrelevant isotype-matched antibodies were used to determine background fluorescence. Data reproducibility was ensured using as instrumental set-up an application setting linked to Cytometer Setup & Tracking Beads (CS&T Beads, BD Biosciences) ran daily. All the experiments were analyzed with FACSDiva (BD Biosciences) or FlowJo (FlowJo LLC, Ashland, USA) softwares.[1,2]

NOTCH1 mutational load

To evaluate *NOTCH1* mutational load, genomic DNA from the c.7541-7542delCT *NOTCH1* mutated cases was amplified with the following primers: forward primer 5'-CCTGGCGGTGCACACACTATTC -3', reverse primer 5'- TGGGAAAGGAAGCCGGGGTCT -3', modified according to Illumina protocol, by using a high fidelity Taq polymerase (Phusion High-Fidelity DNA Polymerase, Thermo Scientific, Milan, Italy). The obtained PCR products were subjected to next generation sequencing (NGS) on MiSeq sequencer (Illumina, San Diego, CA) to obtain a ~1000 coverage-fold for amplicons. Results were expressed as percentage of mutated DNA.

Quantitative real-time PCR (QRT-PCR)

Transcript expression levels of genes of interest (i.e. *MS4A1*, *HES1*, *HES5*, *HDAC1*, *HDAC2*, *NOTCH1* and *B2M*) were evaluated, as reported.[3] For QRT-PCR experiments, primary CLL cases were selected for having >80% of neoplastic cells in the lympho-monocyte fraction. Hydrolysis probes for *MS4A1* (Hs.PT.56a.24784282), *HDAC1* (Hs.PT.58.39528456) and *HDAC2* (Hs.PT.58.3484574) were from Integrated DNA Technologies (IDT, Leuven, Belgium). Taqman Gene Expression assays for *B2M* (Hs00984230_m1), *HES1* (Hs00172878_m1) were from Life Technologies (Monza, Italy). Reactions were done in triplicate from the same cDNA reaction (technical replicates) with FastStart Universal Probe Master (Roche, Milan, Italy) on a CFX96 (Bio-Rad, Milan, Italy) instrument. The relative amount of each gene was calculated utilizing the expression of *B2M* as internal control using the equation $2^{-\Delta Ct}$ where $\Delta Ct=(Ct^{gene}-Ct^{B2M})$.

Western blot (WB)

WB was performed as reported,[4] using the antibodies: anti-cleaved NOTCH1 (Val1744, clone D3B8, CST-Cell Signaling Technology, Leiden, The Netherlands), anti-NOTCH1 (clone D1E11, CST), anti-HDAC1 (clone 10E2, CST), anti-HDAC2 (clone 3F3, CST), anti-CD20 (clone L26, Abcam, Cambridge, UK). Anti-β-actin antibody (clone AC-74, Sigma, Milan, Italy) was used as control. Total proteins were extracted in RIPA lysis buffer (Santa Cruz Biotechnology, Heidelberg, Germany), quantified through Bradford assay (Bio-Rad) and ran in 4-15% SDS-PAGE precast gels (Bio-Rad) prior to transfer to nitrocellulose membranes (Trans-Blot Turbo pack, Bio-Rad). Immunodetection was performed with HRP-conjugated antibodies (Amersham, Milan, Italy) with ClarityECL (Bio-Rad) and Hyperfilm ECL films (Amersham). Films were digitally acquired with an Epson Perfection V330 Photo desktop scanner (Epson, Milan, Italy).

Complement-dependent cytotoxicity (CDC) assay

CDC assay was performed in primary CLL and NICD transfectants, as described.[5] Residual viable cells were evaluated by staining cells with 7-amino-actinomycin-D (BD Biosciences), as described.[2,5] In particular, $2x10^5$ primary CLL cells or NICD transfected MEC-1 cells were incubated with rituximab (5µg/ml) or with ofatunumab (5µg/ml) in a final volume of 150 µl for 10 min at room temperature prior to the addition of PNHS (25%) and a further incubation at 37° C for 1 hour.

Cell culture conditions

MEC1 cells were purchased from DSMZ and maintained at a concentration of $0.5\text{-}2x10^6$ cells/ml in RPMI-1640 (Biochrom, Berlin, Germany) supplemented with 10% heat inactivated fetal bovine serum (Biochrom), 100 U/ml penicillin, 0.1 mg/ml streptomycin and 2 mM L-glutamine (Life Technologies).

NICD plasmids

Plasmids were engineered cloning the NICD coding sequence, derived from the EF.hICN1.CMV.GFP (Addgene plasmid #17623) kind gift from Linzhao Cheng,[6] in a pcDNA3.1-NT-GFP-TOPO scaffold using the TOPO-TA cloning kit (Life Technologies). Site-directed mutagenesis was performed with the Quikchange II XL Mutagenesis kit (Agilent, Milan, Italy). Plasmids were purified with the QiaAmp MIDIprep kit (Qiagen, Milan, Italy).

Transfection with vectors encoding for NICD

MEC-1 cells ($6x10^6$ cells) were transfected with the Amaxa Nucleofector L kit (Lonza, Basel, Switzerland) with 3µg of linearized vector and electroporated (program C-005). Cells were readily resuspended in 2.5ml of pre-warmed RPMI+20%FBS and cultured for four days. Single cell sorting of GFP-positive cells was performed with a FACSAria III cell sorter (BD Biosciences, Milan, Italy). Each cell was seeded in 100µl RPMI+20% FBS and incubated at 37°C. After a week, Geneticin (G418, Life Technologies) was added at a concentration of 500µg/ml for antibiotic selection. Positively transfected clones were evaluated by direct sequencing and western blotting as described above.

In-vitro treatment with pharmaceutical compounds

Purified primary CLL cells, normal B cells and NICD transfected MEC-1 cells ($2x10^6$cells/ml) were treated with the γ-secretase inhibitor (GSI L-685,458, Sigma, 10µM for 6-24 hours) or the HDAC inhibitor 2-propylpentanoic acid (VPA, Depakin, Sanofi, Milan, Italy; 3mM for 48 hours). In control experiments, equal volume of the appropriate solvent compound was added.

Co-immunoprecipitation experiments

Nuclear extracts were obtained as follows: $20x10^6$ cells were collected, resuspended in Nuclear Extract buffer #1 (25mM HEPES, 5mM KCl, 0.5 mM $MgCl_2$, protease inhibitors); one volume of Nuclear Extract buffer #2 (25mM HEPES, 5mM KCl, 0.5 mM $MgCl_2$, protease inhibitors, 1% NP-40) was added and left rotating at 4°C for 15'. After centrifugation, supernatant was removed and nuclei were washed once with Nuclear Extract buffer #3 (25mM HEPES, 5mM KCl, 0.5 mM $MgCl_2$, protease inhibitors, 0.5% NP-40) for 1 hour. Nuclear pellet was then lysed in Nuclear Extract buffer #4 (25mM HEPES, 10% (w/v) Sucrose, 350 mM NaCl, protease inhibitors, 0.01% NP-40) and sonicated with 3 cycles of 30 seconds in a Biorupture sonicator (Diagenode, Liege, Belgium). Lysates were quantified by Bradford assay (Bio-Rad). Co-immunoprecipitation was performed with Protein G-Mag Sepharose beads (GE healthcare, Milan, Italy) according to manufacturer's protocol and western blotting was performed as described above. Image acquisition

of co-immunoprecipitation western blots was performed using ImageQuant LAS4000 and TL Version 7.0 software (GE Healthcare).

Chromatin immunoprecipitation (ChIP) assay

Cells ($40x10^6$) were cross-linked with 1% formaldehyde and lysed according to the protocol. DNA was digested with 1µl Micrococcal nuclease (kit provided) to a fragment size from 150 to 900 base pairs. Seven µg of cross-linked chromatin were used to perform immunoprecipitation. The same primers used for qualitative PCR were used for QRT-PCR using Sso Fast Evagreen Supermix (Bio-Rad). Quantification of *MS4A1* promoter DNA bound to immunoprecipitated HDAC1 or HDAC2 was determined using the Percent Input Method according to the equation: Percent input= 2% x $2^{(Ct\ 2\%\ Input\ Sample - Ct\ IP\ Sample)}$.

Statistical analysis

All statistical analyses were performed with Medcalc software (Medcalc Software, Ostend, Belgium). Reported values for experiments using NICD transfected cells including CDC assay, treatment with pharmaceutical compounds (i.e. GSI and VPA) and ChIP assay were an average of three independent experiments. Data are presented as Tukey box-and-whiskers plots or, alternatively, data are presented as histograms, indicating the mean ± standard error mean (SEM). In the text, data are presented as mean ± SEM. Data were compared using Student's t-test for independent or paired samples.

References

1 Gattei V, Zucchetto A, Russo S, Stefanon A, Bomben R, Dal Bo M *et al*. Immunophenotypic clustering of B-CLL identifies subsets with different prognosis without a strict correlation with IgVH mutational status and CD38 expression. Blood 102, 667a. 2003.
Ref Type: Abstract

2 Zucchetto A, Vaisitti T, Benedetti D, Tissino E, Bertagnolo V, Rossi D *et al*. The CD49d/CD29 complex is physically and functionally associated with CD38 in B-cell chronic lymphocytic leukemia cells. *Leukemia* 2012; **26**: 1301-1312.

3 Bomben R, Dal-Bo M, Benedetti D, Capello D, Forconi F, Marconi D *et al*. Expression of mutated IGHV3-23 genes in chronic lymphocytic leukemia identifies a disease subset with peculiar clinical and biological features. *Clin Cancer Res* 2010; **16**: 620-628.

4 Pozzo F, Dal BM, Peragine N, Bomben R, Zucchetto A, Rossi F *et al*. Detection of TP53 dysfunction in chronic lymphocytic leukemia by an in vitro functional assay based on TP53 activation by the non-genotoxic drug Nutlin-3: a proposal for clinical application. *J Hematol Oncol* 2013; **6**: 83.

5 Macor P, Tripodo C, Zorzet S, Piovan E, Bossi F, Marzari R *et al*. In vivo targeting of human neutralizing antibodies against CD55 and CD59 to lymphoma cells increases the antitumor activity of rituximab. *Cancer Res* 2007; **67**: 10556-10563.

6 Yu X, Alder JK, Chun JH, Friedman AD, Heimfeld S, Cheng L *et al*. HES1 inhibits cycling of hematopoietic progenitor cells via DNA binding. *Stem Cells* 2006; **24**: 876-888.

Table S1. Biological characterization of the CLL cohort (692 cases).

ID #	*NOTCH1* status[a]	*IGHV* status[b]	FISH status[c]	CD49d[d]	CD38[d]	ZAP-70[d,e]	CD20 MFI[f]	Anti-CD20 antibody[g]
1	wt	m	del13p	1.4	2.0	1.0	7188	FITC
2	mut	um	norm	28.6	89.9	22.0	4258	FITC
3	wt	um	del13p	36.6	6.0	23.0	1294	FITC
4	mut	m	del13p	6.0	5.0	19.0	5057	FITC
5	wt	m	del13p	4.8	7.4	6.0	5373	FITC
6	wt	m	del13p	99.9	2.0	22.0	8169	FITC
7	wt	m	del13p	1.0	1.0	11.0	1668	FITC
8	wt	m	tris12	100.0	10.0	25.0	25468	FITC
9	wt	um	del13p	72.0	4.5	33.0	4815	FITC
10	wt	um	tris12	9.0	5.0	29.0	2987	FITC
11	wt	m	del13p	4.0	5.0	14.0	3115	FITC
12	wt	m	norm	4.0	2.0	42.0	2769	FITC
13	wt	m	norm	8.6	2.3	57.0	2925	FITC
14	wt	m	del13p	43.4	4.6	70.0	4822	FITC
15	wt	m	tris12	98.0	18.0	30.0	29097	FITC
16	wt	m	norm	6.0	2.0	19.0	2290	FITC
17	wt	m	del13p	1.0	2.0	53.0	5276	FITC
18	wt	m	del13p	1.0	1.0	20.0	2093	FITC
19	wt	m	del17p	2.6	1.0	8.0	2368	FITC
20	wt	um	norm	90.8	84.0	33.0	1767	FITC
21	wt	um	del13p	81.6	5.0	27.0	7866	FITC
22	wt	m	del13p	7.0	2.0	12.0	7431	FITC
23	wt	m	del13p	1.0	1.0	1.0	2082	FITC
24	wt	n.a.	del13p	1.0	1.0	10.0	1288	FITC
25	wt	m	del13p	2.7	1.0	6.0	1954	FITC
26	mut	um	norm	53.8	74.7	53.0	1882	FITC
27	wt	um	del13p	9.0	4.6	34.0	3213	FITC
28	wt	m	del13p	1.0	1.0	55.0	3064	FITC
29	wt	um	norm	99.0	19.4	59.0	3720	FITC
30	wt	m	norm	82.0	30.4	74.0	4600	FITC
31	wt	m	norm	99.3	16.5	69.0	2797	FITC
32	wt	m	del13p	18.0	5.5	68.0	3520	FITC
33	wt	m	norm	2.3	1.0	52.0	2380	FITC
34	mut	m	del13p	1.0	4.0	38.0	3685	FITC
35	wt	um	tris12	98.0	56.6	50.0	2065	FITC
36	wt	n.a.	del17p	1.0	4.0	20.0	1640	FITC
37	wt	m	del13p	8.2	2.7	19.0	2320	FITC
38	wt	um	del13p	98.7	8.0	21.0	1108	FITC
39	wt	m	norm	7.0	7.0	29.0	2386	FITC
40	wt	m	norm	10.0	10.0	25.0	2546	FITC
41	wt	m	del13p	2.7	9.2	25.0	3109	FITC
42	wt	um	del13p	1.0	16.3	16.0	2172	FITC
43	wt	um	del17p	50.0	63.0	34.0	1945	FITC
44	wt	m	del13p	8.0	4.0	28.0	3069	FITC
45	wt	m	del13p	3.0	4.0	15.0	2808	FITC
46	wt	m	del13p	1.3	8.0	27.0	1741	FITC
47	wt	um	del13p	80.0	50.0	28.0	2264	FITC

48	mut	um	norm	1.0	59.0	69.0	3569	FITC
49	wt	m	norm	25.0	20.6	25.0	1584	FITC
50	wt	um	del11q	99.0	33.6	57.0	3152	FITC
51	wt	um	norm	4.3	8.0	55.0	2506	FITC
52	wt	m	norm	6.5	6.0	48.0	2300	FITC
53	mut	um	del11q	8.3	96.2	40.0	2297	FITC
54	wt	m	norm	40.2	45.0	24.0	10889	FITC
55	wt	m	norm	66.0	80.9	19.0	6564	FITC
56	wt	um	del11q	1.0	1.0	50.0	3595	FITC
57	wt	um	del11q	14.0	36.8	32.0	2624	FITC
58	wt	m	del13p	1.0	8.8	26.0	2027	FITC
59	wt	m	del13p	76.0	1.0	32.0	2615	FITC
60	wt	m	del13p	3.0	5.8	42.0	1380	FITC
61	wt	m	del13p	99.9	25.0	25.0	9638	FITC
62	mut	um	tris12	98.4	77.3	70.0	2189	FITC
63	wt	um	norm	98.0	59.6	42.0	4138	FITC
64	wt	m	norm	5.4	1.4	35.0	2378	FITC
65	wt	um	del17p	1.5	6.0	22.0	1773	FITC
66	wt	m	tris12	96.3	49.6	50.0	26131	FITC
67	wt	m	del13p	2.0	2.0	17.0	1939	FITC
68	wt	um	del11q	1.0	1.0	12.0	2481	FITC
69	wt	m	tris12	99.7	88.9	80.0	16810	FITC
70	wt	um	tris12	93.0	21.4	68.0	2477	FITC
71	wt	um	del11q	1.2	96.0	70.0	3181	FITC
72	wt	um	del13p	1.0	3.0	27.0	4808	FITC
73	wt	m	del13p	12.0	7.0	49.0	3489	FITC
74	wt	um	del13p	2.0	3.4	59.0	1600	FITC
75	mut	m	del13p	4.0	3.9	49.0	4548	FITC
76	wt	m	del13p	3.0	6.0	19.0	1894	FITC
77	wt	m	del13p	7.6	2.0	n.a.	3512	FITC
78	mut	um	tris12	70.0	23.0	n.a.	3126	FITC
79	wt	um	del13p	1.0	37.0	n.a.	1721	FITC
80	wt	um	norm	4.5	2.0	23.0	1651	FITC
81	wt	m	del13p	1.0	1.0	37.0	1356	FITC
82	wt	m	del13p	1.0	1.0	53.0	3865	FITC
83	wt	m	del13p	1.9	15.0	26.0	1583	FITC
84	wt	m	tris12	100.0	95.0	52.0	25248	FITC
85	wt	um	del13p	1.0	15.5	40.0	804	FITC
86	wt	m	norm	9.0	15.0	44.0	5983	FITC
87	wt	m	del13p	12.5	10.0	60.0	3812	FITC
88	wt	m	del13p	96.2	17.0	43.0	3528	FITC
89	wt	n.a.	del17p	4.0	17.6	13.0	4950	FITC
90	wt	m	del13p	15.0	15.0	52.0	2549	FITC
91	wt	m	del11q	9.0	5.0	36.0	4420	FITC
92	wt	m	tris12	87.0	51.4	31.0	14291	FITC
93	wt	m	del17p	1.0	14.0	29.0	1833	FITC
94	wt	m	del13p	6.0	10.0	44.0	2054	FITC
95	mut	m	tris12	99.6	7.0	52.0	4048	FITC
96	wt	m	tris12	100.0	95.0	40.0	5402	FITC
97	mut	um	tris12	21.6	49.0	86.0	1251	FITC
98	wt	um	norm	2.0	7.0	68.0	1037	FITC
99	wt	m	tris12	100.0	22.0	74.0	7621	FITC

100	wt	um	norm	10.0	2.0	40.0	1160	FITC
101	wt	m	del17p	3.0	5.0	26.0	1995	FITC
102	wt	m	del13p	1.0	3.0	10.0	506	FITC
103	mut	um	del17p	84.5	82.6	69.0	1831	FITC
104	mut	um	norm	92.4	31.4	50.0	472	FITC
105	mut	um	del17p	95.0	62.5	39.0	1510	FITC
106	wt	um	norm	49.3	97.7	70.0	573	FITC
107	mut	m	norm	1.6	39.5	78.0	564	FITC
108	wt	m	norm	9.0	20.0	56.0	1377	FITC
109	wt	um	del13p	1.0	2.6	60.0	1844	FITC
110	wt	m	del13p	37.0	5.9	35.0	2090	FITC
111	wt	m	norm	33.4	1.7	65.0	1359	FITC
112	wt	m	norm	40.1	5.4	33.0	963	FITC
113	mut	um	norm	53.3	1.0	23.0	228	FITC
114	wt	m	norm	100.0	3.3	6.0	3255	FITC
115	wt	um	del13p	98.4	71.7	57.0	1085	FITC
116	wt	um	norm	96.8	99.7	50.0	8508	FITC
117	wt	m	del13p	1.5	9.7	22.0	984	FITC
118	wt	m	del13p	1.0	17.0	63.0	3804	FITC
119	wt	m	norm	58.1	3.1	33.0	1541	FITC
120	mut	um	tris12	62.1	17.1	46.0	2683	FITC
121	wt	m	del17p	1.0	3.0	23.0	1602	FITC
122	mut	um	tris12	43.6	35.1	28.0	762	FITC
123	wt	um	del11q	29.0	9.3	58.0	478	FITC
124	wt	um	tris12	98.0	40.0	82.0	4192	FITC
125	wt	m	norm	9.8	6.7	23.0	3234	FITC
126	wt	n.a.	del13p	1.4	1.9	14.0	2426	FITC
127	wt	m	norm	3.3	4.0	18.0	825	FITC
128	wt	um	del11q	41.1	78.3	21.0	521	FITC
129	wt	m	del13p	1.5	1.0	26.0	1514	FITC
130	wt	m	tris12	13.0	9.3	31.0	1734	FITC
131	wt	m	tris12	4.9	14.3	42.0	901	FITC
132	wt	m	tris12	99.8	98.8	49.0	5737	FITC
133	wt	um	del11q	1.0	60.4	59.0	944	FITC
134	wt	um	del13p	1.0	50.2	39.0	3699	FITC
135	wt	m	norm	37.6	20.1	19.0	963	FITC
136	wt	m	norm	100.0	35.0	51.0	11136	FITC
137	wt	m	del13p	1.0	2.2	10.0	1885	FITC
138	wt	m	norm	96.6	15.9	43.0	6778	FITC
139	mut	um	tris12	86.8	24.2	78.0	1260	FITC
140	wt	m	del13p	94.4	1.1	27.0	561	FITC
141	wt	um	del17p	59.6	13.4	50.0	1326	FITC
142	wt	um	tris12	99.8	23.2	49.0	10704	FITC
143	wt	m	del13p	1.3	3.3	20.0	1218	FITC
144	mut	um	del11q	9.0	16.5	80.0	958	FITC
145	wt	m	del13p	2.2	5.0	50.0	1472	FITC
146	mut	um	tris12	87.0	43.3	87.0	1602	FITC
147	mut	n.a.	norm	81.2	33.3	53.0	1687	FITC
148	wt	n.a.	tris12	97.3	6.5	52.0	560	FITC
149	wt	m	norm	8.0	4.9	44.0	801	FITC
150	wt	m	norm	1.7	1.9	59.0	695	FITC
151	wt	um	del17p	2.1	35.6	75.0	525	FITC

152	wt	m	norm	56.3	8.1	47.0	834	FITC
153	wt	m	del13p	1.0	2.3	70.0	2076	FITC
154	wt	um	tris12	80.9	98.5	90.0	2395	FITC
155	wt	um	norm	99.7	18.3	40.0	904	FITC
156	wt	m	del13p	1.0	1.6	13.0	1621	FITC
157	wt	m	del13p	14.7	5.4	47.0	1296	FITC
158	wt	m	del13p	1.9	2.7	72.0	568	FITC
159	wt	m	norm	29.7	1.0	39.0	434	FITC
160	wt	m	del13p	18.8	3.6	81.0	2049	FITC
161	wt	um	tris12	92.7	16.1	80.0	5533	FITC
162	wt	m	del13p	1.0	2.7	60.0	996	FITC
163	mut	m	del13p	35.4	9.9	89.0	2691	FITC
164	wt	m	del17p	47.2	3.2	70.0	1469	FITC
165	wt	um	norm	5.6	35.7	66.0	1194	FITC
166	wt	m	norm	1.0	5.1	60.0	711	FITC
167	wt	um	del13p	4.2	42.8	38.0	1121	FITC
168	wt	um	tris12	96.5	45.5	64.0	5670	FITC
169	wt	m	del17p	1.3	13.9	41.0	3321	FITC
170	mut	m	tris12	20.0	7.0	61.0	1999	FITC
171	mut	um	tris12	93.9	42.3	72.0	1620	FITC
172	wt	um	norm	69.0	30.8	78.0	642	FITC
173	mut	um	del13p	1.0	18.9	54.0	785	FITC
174	wt	m	norm	98.9	3.9	37.0	646	FITC
175	mut	um	tris12	99.9	57.0	52.0	1875	FITC
176	mut	um	del13p	97.4	48.6	58.0	978	FITC
177	wt	um	tris12	31.1	10.3	58.0	186	FITC
178	wt	m	del13p	1.1	2.3	10.0	205	FITC
179	wt	m	del13p	2.0	2.2	20.0	1957	FITC
180	wt	m	del13p	4.0	7.6	19.0	3616	FITC
181	wt	m	del13p	5.0	1.0	5.0	698	FITC
182	wt	m	del13p	11.0	2.0	3.0	1255	FITC
183	wt	m	tris12	99.9	4.0	5.0	10801	FITC
184	wt	um	del17p	11.5	35.0	20.0	1904	FITC
185	mut	um	del13p	93.9	36.9	19.0	41	FITC
186	wt	m	tris12	97.3	28.7	26.0	9336	FITC
187	wt	m	del13p	1.7	3.8	14.0	713	FITC
188	wt	m	del13p	1.2	9.1	22.0	1038	FITC
189	wt	m	norm	9.3	14.5	38.0	1132	FITC
190	wt	um	tris12	64.8	8.9	68.0	1516	FITC
191	mut	um	del13p	2.9	53.4	60.3	2238	FITC
192	wt	m	tris12	88.9	24.0	19.4	6021	FITC
193	wt	m	del13p	2.4	2.2	14.8	1783	FITC
194	wt	um	del11q	7.7	3.3	35.2	1956	FITC
195	wt	m	del13p	2.3	2.0	1.6	419	FITC
196	wt	m	del13p	4.0	4.6	3.6	2184	FITC
197	wt	um	del13p	6.2	6.2	5.3	2437	FITC
198	wt	um	norm	6.5	5.9	17.6	752	FITC
199	wt	um	del11q	2.6	59.9	40.7	1413	FITC
200	wt	m	del13p	2.3	8.5	6.3	1408	FITC
201	wt	um	norm	97.6	82.6	13.1	3187	FITC
202	wt	um	norm	88.1	57.5	90.2	709	FITC
203	wt	um	tris12	84.0	89.6	37.3	4137	FITC

204	wt	um	del11q	1.7	76.0	81.2	2355	FITC
205	wt	um	norm	2.9	49.2	20.0	1478	FITC
206	wt	m	del13p	11.3	1.3	6.0	993	FITC
207	wt	m	norm	1.0	1.0	7.0	1639	FITC
208	wt	um	del13p	4.9	7.0	45.0	1210	FITC
209	wt	m	norm	14.1	35.1	30.0	1207	FITC
210	wt	n.a.	norm	6.3	32.7	26.0	368	FITC
211	wt	m	del13p	26.9	3.3	4.0	3053	FITC
212	wt	um	del11q	1.1	7.4	23.0	411	FITC
213	wt	m	del13p	1.0	7.4	36.0	2415	FITC
214	mut	um	del13p	1.0	1.1	40.0	858	FITC
215	wt	um	norm	51.0	49.0	29.0	957	FITC
216	wt	m	norm	4.4	5.9	16.0	1094	FITC
217	wt	m	del13p	1.6	4.4	18.6	739	FITC
218	mut	um	tris12	42.9	47.4	38.0	1444	FITC
219	wt	m	del13p	5.5	3.7	19.0	1339	FITC
220	wt	m	norm	1.0	1.4	11.0	578	FITC
221	wt	m	del13p	3.4	6.0	19.0	1962	FITC
222	wt	m	norm	1.5	2.3	1.0	1233	FITC
223	wt	m	norm	1.0	63.8	13.7	751	FITC
224	mut	um	del13p	3.7	64.7	20.0	601	FITC
225	wt	m	tris12	100.0	99.9	15.0	10857	FITC
226	wt	m	del13p	76.2	5.8	20.0	2254	FITC
227	wt	m	del13p	1.2	2.0	29.9	2526	FITC
228	wt	m	del13p	99.9	8.4	56.0	14634	FITC
229	wt	um	norm	60.6	16.6	58.0	793	FITC
230	wt	m	del13p	18.1	3.6	18.0	1230	FITC
231	wt	m	del13p	91.1	2.8	47.0	2003	FITC
232	wt	m	del13p	100.0	3.1	50.0	10987	FITC
233	mut	um	del11q	1.0	4.2	52.0	3068	FITC
234	wt	um	del13p	1.7	1.2	30.0	1391	FITC
235	wt	m	del13p	2.9	5.8	52.0	1524	FITC
236	wt	m	del13p	1.0	7.8	34.0	2707	FITC
237	wt	m	tris12	89.8	37.1	20.0	10278	FITC
238	wt	m	del13p	1.0	1.4	9.0	2260	FITC
239	wt	m	del13p	8.5	7.7	32.0	3220	FITC
240	wt	m	del11q	26.2	82.3	49.0	3981	FITC
241	wt	m	del13p	4.0	1.0	6.0	1155	FITC
242	wt	um	norm	78.0	43.2	55.0	3447	FITC
243	mut	m	tris12	21.0	31.6	31.0	2128	FITC
244	mut	um	del17p	99.7	27.2	17.0	2637	FITC
245	wt	m	norm	23.0	2.6	7.0	1163	FITC
246	wt	m	tris12	98.0	98.5	22.0	6231	FITC
247	wt	m	norm	4.3	3.0	6.5	2969	FITC
248	wt	m	del13p	4.3	5.2	31.0	2422	FITC
249	wt	m	del13p	1.9	2.4	12.3	3289	FITC
250	wt	m	del13p	1.0	1.0	4.6	1572	FITC
251	wt	m	del17p	1.9	1.0	11.0	548	FITC
252	wt	m	norm	12.5	54.2	20.1	989	FITC
253	wt	m	norm	1.0	32.0	53.5	665	FITC
254	wt	m	del13p	100.0	98.1	22.9	2020	FITC
255	wt	m	del13p	4.5	4.2	12.9	2950	FITC

256	wt	m	del13p	1.9	7.0	10.1	1205	FITC
257	wt	m	norm	6.6	3.2	19.0	1185	FITC
258	wt	m	del13p	100.0	2.0	9.0	2424	FITC
259	wt	um	tris12	76.5	89.1	63.0	1953	FITC
260	wt	m	norm	96.7	72.3	50.1	2251	FITC
261	wt	m	del13p	10.1	6.0	9.8	1883	FITC
262	wt	um	norm	5.7	4.7	36.0	1163	FITC
263	wt	um	del17p	3.7	7.4	45.0	697	FITC
264	mut	um	norm	100.0	98.0	42.0	2473	FITC
265	wt	m	del13p	5.0	2.8	18.0	1659	FITC
266	mut	um	tris12	98.5	98.5	75.0	604	FITC
267	wt	m	norm	2.2	1.4	19.0	1638	FITC
268	wt	um	del13p	1.8	3.7	27.0	1586	FITC
269	mut	um	tris12	69.3	55.0	42.0	2432	FITC
270	wt	um	del11q	1.7	17.4	19.0	2366	FITC
271	wt	um	norm	2.0	19.5	19.0	2743	FITC
272	wt	um	del13p	1.3	1.7	7.0	1700	FITC
273	wt	um	tris12	27.0	11.9	5.0	622	FITC
274	wt	um	norm	98.5	88.2	35.0	3195	FITC
275	wt	m	del13p	96.2	57.3	18.0	1808	FITC
276	wt	um	tris12	97.0	77.0	38.0	3374	FITC
277	wt	n.a.	del13p	8.1	6.4	4.0	2136	FITC
278	wt	m	norm	100.0	94.8	9.0	10364	FITC
279	wt	m	norm	42.6	16.5	19.0	3822	FITC
280	wt	m	del13p	4.6	5.3	2.0	3175	FITC
281	wt	um	norm	98.5	85.0	77.0	3902	FITC
282	wt	um	del11q	1.8	63.1	29.0	1076	FITC
283	wt	m	norm	99.9	2.2	1.0	7829	FITC
284	wt	um	del11q	7.0	50.7	23.0	1800	FITC
285	wt	um	del13p	1.6	2.4	15.0	628	FITC
286	wt	m	del13p	4.1	4.7	27.0	2453	FITC
287	wt	m	del13p	1.3	1.9	1.0	1128	FITC
288	wt	um	del13p	1.0	65.0	26.0	3874	FITC
289	wt	um	del17p	27.7	74.3	26.0	2227	FITC
290	wt	n.a.	del13p	5.1	2.4	14.0	1650	FITC
291	wt	m	del13p	8.1	7.6	40.0	1680	FITC
292	wt	m	norm	6.5	9.1	14.0	2168	FITC
293	wt	n.a.	del17p	1.2	13.4	61.0	4669	FITC
294	wt	m	tris12	98.8	33.2	19.0	4053	FITC
295	wt	um	norm	1.0	1.8	28.0	1068	FITC
296	wt	um	tris12	94.9	11.0	77.0	1450	FITC
297	wt	um	norm	3.1	2.2	19.0	2305	FITC
298	mut	um	norm	97.3	95.9	38.5	1682	FITC
299	wt	um	del11q	49.6	66.7	33.0	1471	FITC
300	wt	um	norm	92.6	1.0	19.6	2847	FITC
301	wt	n.a.	norm	1.0	6.2	13.0	1450	FITC
302	wt	m	del13p	10.3	1.9	2.0	1362	FITC
303	mut	m	norm	99.2	40.1	12.0	2182	FITC
304	mut	um	tris12	89.3	10.5	37.0	881	FITC
305	mut	um	del13p	86.7	67.8	36.0	2136	FITC
306	wt	um	tris12	92.4	84.5	31.0	3111	FITC
307	wt	um	norm	9.8	22.4	32.0	391	FITC

308	wt	m	del13p	6.1	4.2	19.0	1801	FITC
309	wt	m	tris12	100.0	98.7	12.0	11468	FITC
310	wt	n.a.	del13p	4.1	5.2	19.0	949	FITC
311	wt	m	tris12	91.6	7.0	28.0	5943	FITC
312	wt	n.a.	del13p	2.7	4.7	6.0	1709	FITC
313	wt	m	del11q	33.5	11.6	26.0	2360	FITC
314	wt	m	norm	2.6	1.3	10.0	3772	FITC
315	wt	n.a.	del13p	1.5	89.3	19.0	655	FITC
316	wt	um	del13p	78.7	3.6	19.0	1350	FITC
317	wt	um	del13p	28.5	7.4	30.0	2484	FITC
318	wt	n.a.	norm	54.5	95.2	16.0	3391	FITC
319	wt	um	tris12	100.0	88.0	18.0	8648	FITC
320	wt	um	del11q	1.0	1.6	21.0	1085	FITC
321	wt	m	del13p	8.4	63.3	21.0	3246	FITC
322	wt	m	del13p	11.7	5.1	20.0	1572	FITC
323	wt	um	del13p	18.2	31.9	23.0	1168	FITC
324	wt	m	del13p	6.5	1.6	19.0	1285	FITC
325	wt	m	tris12	99.8	82.1	33.0	8510	FITC
326	wt	m	del13p	11.5	5.6	17.0	4678	FITC
327	wt	m	norm	81.3	2.3	8.0	1968	FITC
328	wt	um	del13p	1.9	1.0	44.0	1430	FITC
329	wt	n.a.	del17p	25.9	50.7	32.0	1896	FITC
330	wt	um	tris12	95.2	75.3	42.0	1062	FITC
331	wt	n.a.	norm	30.2	5.6	12.0	2014	FITC
332	wt	m	tris12	100.0	9.1	1.0	12251	FITC
333	wt	m	norm	9.9	3.0	5.0	1129	FITC
334	wt	m	del13p	46.2	69.1	48.0	2664	FITC
335	wt	n.a.	del13p	23.2	1.9	32.0	2216	FITC
336	wt	m	del13p	70.1	3.1	10.0	1661	FITC
337	wt	m	del13p	9.7	4.1	20.0	2075	FITC
338	wt	m	norm	29.4	3.9	7.0	1469	FITC
339	wt	m	norm	35.7	5.5	13.0	2263	FITC
340	mut	um	del13p	97.9	29.6	20.0	558	FITC
341	wt	m	del13p	23.5	8.3	8.0	772	FITC
342	wt	m	norm	47.6	33.3	3.0	1350	FITC
343	wt	m	norm	100.0	2.3	5.0	15024	FITC
344	wt	um	tris12	89.1	76.1	43.0	3031	FITC
345	wt	um	tris12	100.0	3.8	46.0	7355	FITC
346	wt	um	del11q	3.2	2.5	8.0	890	FITC
347	mut	n.a.	del13p	3.7	3.0	9.0	2654	FITC
348	wt	um	del13p	4.7	5.5	9.0	234	FITC
349	wt	n.a.	norm	21.3	4.4	30.0	1281	FITC
350	wt	m	del13p	17.5	4.0	10.0	3385	FITC
351	wt	um	del11q	83.9	45.9	53.0	1720	FITC
352	wt	m	del13p	10.8	1.1	2.0	1543	FITC
353	wt	m	tris12	22.5	96.7	3.0	2460	FITC
354	wt	um	tris12	87.0	28.1	48.0	4008	FITC
355	wt	um	del13p	2.6	53.1	32.0	2289	FITC
356	wt	m	del13p	10.4	4.5	18.0	2030	FITC
357	wt	um	tris12	54.2	38.9	24.0	2382	FITC
358	wt	m	del13p	83.2	1.2	n.a.	882	FITC
359	wt	um	norm	6.5	24.5	n.a.	2796	FITC

360	wt	m	del13p	1.5	1.5	7.0	1817	FITC
361	wt	um	norm	59.6	58.8	24.0	1786	FITC
362	wt	m	del13p	10.3	7.9	19.0	3301	FITC
363	wt	um	norm	66.1	18.7	22.0	1542	FITC
364	wt	um	del11q	16.2	83.7	49.0	2212	FITC
365	mut	um	tris12	100.0	23.6	74.0	989	FITC
366	wt	um	del11q	22.0	26.8	3.0	3664	FITC
367	wt	um	del17p	66.5	6.7	8.0	24	FITC
368	wt	m	norm	99.9	7.2	2.0	9491	FITC
369	mut	um	norm	99.6	86.8	68.0	2824	FITC
370	wt	m	del13p	46.5	8.4	35.0	5189	FITC
371	wt	um	tris12	70.0	23.0	12.0	6035	FITC
372	wt	m	tris12	99.9	51.6	2.0	10871	FITC
373	wt	um	del11q	15.5	98.6	25.0	4270	FITC
374	wt	um	del17p	38.8	79.8	47.0	653	FITC
375	wt	um	norm	86.8	38.2	36.0	2328	FITC
376	wt	m	norm	3.3	25.4	2.0	759	FITC
377	wt	m	norm	1.0	1.5	10.0	1644	FITC
378	wt	m	tris12	100.0	20.2	16.0	16209	FITC
379	mut	m	del13p	22.5	1.0	19.0	1526	FITC
380	wt	m	norm	2.5	5.9	17.0	1467	FITC
381	wt	n.a.	norm	2.5	1.0	15.0	1121	FITC
382	wt	m	tris12	13.2	1.0	11.0	1683	FITC
383	mut	um	tris12	32.3	14.7	52.0	1904	FITC
384	wt	m	del13p	1.0	1.0	15.0	1730	FITC
385	wt	um	tris12	93.4	93.0	62.0	10444	FITC
386	wt	um	tris12	81.0	77.3	45.0	2255	FITC
387	wt	um	tris12	74.1	16.2	59.0	2469	FITC
388	wt	m	del13p	11.0	6.3	1.0	2125	FITC
389	wt	m	del11q	4.5	82.0	1.0	1095	FITC
390	wt	m	del13p	1.8	2.9	11.0	996	FITC
391	wt	um	del13p	62.4	5.5	26.0	1767	FITC
392	wt	m	tris12	100.0	54.4	19.0	7258	FITC
393	wt	m	del13p	1.0	2.0	18.0	1026	FITC
394	wt	um	norm	1.0	16.0	98.0	234	FITC
395	wt	um	del11q	1.0	1.5	44.0	2188	FITC
396	wt	um	del17p	16.5	3.6	16.0	1053	FITC
397	wt	m	norm	20.0	6.0	5.0	2681	FITC
398	wt	um	norm	7.0	13.0	29.0	1650	FITC
399	wt	um	norm	36.9	16.3	13.0	1569	FITC
400	wt	m	del13p	10.0	3.5	20.0	2356	FITC
401	wt	m	del13p	1.0	1.0	15.0	4434	FITC
402	wt	m	del13p	3.0	10.0	n.a.	1695	FITC
403	wt	m	tris12	99.5	6.0	n.a.	4270	FITC
404	wt	um	norm	97.5	12.4	n.a.	697	FITC
405	wt	um	tris12	98.0	99.0	44.0	2776	FITC
406	mut	um	norm	98.0	49.0	60.0	478	FITC
407	wt	n.a.	norm	100.0	21.0	50.0	11517	FITC
408	mut	um	del17p	94.5	7.6	19.0	21	FITC
409	wt	um	tris12	7.9	3.1	32.0	522	FITC
410	wt	um	del11q	92.3	23.0	40.0	81	FITC
411	wt	um	tris12	88.1	5.1	n.a.	1575	FITC

412	wt	um	del11q	1.9	3.5	n.a.	3486	FITC
413	wt	m	del13p	1.0	1.0	30.0	1017	FITC
414	wt	m	del13p	4.4	1.0	31.0	1632	FITC
415	wt	m	del17p	1.0	52.0	19.0	3011	FITC
416	wt	m	del13p	1.0	1.0	1.0	2316	FITC
417	wt	n.a.	del11q	6.0	55.7	33.0	2806	FITC
418	wt	m	norm	21.8	49.6	8.0	3284	FITC
419	wt	um	del13p	93.6	3.6	17.0	1830	FITC
420	mut	um	tris12	88.9	43.4	40.0	3100	FITC
421	wt	m	tris12	36.2	39.1	n.a.	9848	FITC
422	wt	m	del17p	60.8	62.8	26.0	2356	FITC
423	wt	m	del13p	10.4	3.1	7.0	2875	FITC
424	wt	um	del17p	99.5	79.7	21.0	3091	FITC
425	wt	m	norm	22.6	15.2	31.0	2287	FITC
426	wt	m	del13p	5.8	1.0	28.0	3160	FITC
427	wt	m	tris12	100.0	88.2	10.0	19559	FITC
428	mut	m	del17p	2.8	10.6	15.0	615	FITC
429	wt	um	tris12	96.4	94.6	42.0	1202	FITC
430	wt	um	del13p	14.9	19.7	19.0	1655	FITC
431	mut	um	del11q	2.8	87.8	n.a.	2481	FITC
432	wt	n.a.	del11q	97.9	61.4	37.0	1438	FITC
433	wt	um	del13p	1.2	3.2	16.1	2624	FITC
434	wt	um	del17p	3.2	6.5	41.3	2052	FITC
435	wt	m	del13p	8.9	6.6	23.8	2644	FITC
436	wt	m	del13p	2.9	2.0	2.0	1159	FITC
437	wt	n.a.	tris12	33.7	1.2	8.7	2861	FITC
438	wt	um	del13p	9.1	65.6	22.0	2652	FITC
439	wt	um	del11q	3.0	77.3	23.5	2127	FITC
440	wt	n.a.	del13p	32.6	5.9	14.4	953	FITC
441	wt	m	del13p	2.7	2.5	16.7	632	FITC
442	mut	um	tris12	94.8	47.2	24.5	1977	FITC
443	wt	n.a.	norm	12.4	15.9	13.0	1784	FITC
444	wt	n.a.	del11q	2.1	5.0	2.5	1256	FITC
445	wt	m	del17p	81.1	7.6	5.4	1874	FITC
446	wt	um	tris12	36.5	8.8	n.a.	904	FITC
447	wt	m	del13p	8.7	13.5	n.a.	1048	FITC
448	wt	um	del13p	6.3	4.0	n.a.	1964	FITC
449	wt	m	del13p	1.8	1.5	n.a.	1435	FITC
450	wt	um	del13p	5.8	18.5	n.a.	2933	FITC
451	wt	m	del13p	5.0	1.2	9.0	1435	FITC
452	wt	m	del13p	1.8	2.6	n.a.	1901	FITC
453	wt	n.a.	del11q	98.8	69.2	n.a.	2396	FITC
454	wt	m	del13p	7.0	6.7	n.a.	2906	FITC
455	wt	m	del13p	5.7	4.9	n.a.	2052	FITC
456	wt	m	norm	4.6	2.4	n.a.	2686	FITC
457	wt	m	del13p	86.2	96.9	n.a.	3610	FITC
458	mut	um	del13p	13.2	87.7	n.a.	1273	FITC
459	wt	m	norm	24.0	1.0	n.a.	3626	FITC
460	wt	n.a.	del13p	57.1	31.5	n.a.	1994	FITC
461	mut	n.a.	del17p	39.1	70.7	n.a.	507	FITC
462	wt	um	del13p	59.4	1.0	n.a.	1064	FITC
463	wt	m	del13p	1.0	1.3	n.a.	1798	FITC

464	wt	m	norm	4.6	8.1	n.a.	809	FITC
465	wt	m	tris12	99.9	6.0	n.a.	19829	FITC
466	wt	m	norm	6.0	4.5	n.a.	2141	FITC
467	wt	um	del11q	1.4	9.0	n.a.	2844	FITC
468	wt	n.a.	del13p	9.4	1.1	n.a.	654	FITC
469	wt	m	norm	6.7	7.1	n.a.	1542	FITC
470	wt	um	norm	2.0	67.3	n.a.	3043	FITC
471	wt	m	del13p	8.2	11.2	n.a.	2140	FITC
472	wt	m	del13p	1.0	1.6	n.a.	1853	FITC
473	wt	um	tris12	98.4	64.6	n.a.	2438	FITC
474	wt	n.a.	del13p	15.8	5.3	n.a.	1566	FITC
475	wt	m	del13p	99.7	22.4	n.a.	15758	FITC
476	mut	n.a.	norm	86.9	63.5	n.a.	3683	FITC
477	wt	m	del13p	96.6	57.6	n.a.	3470	FITC
478	wt	m	norm	16.0	1.0	n.a.	1471	FITC
479	wt	um	del11q	5.5	23.6	n.a.	1820	FITC
480	wt	m	norm	18.0	84.3	n.a.	807	FITC
481	wt	m	del13p	100.0	1.6	n.a.	10082	FITC
482	wt	um	del11q	8.0	99.1	n.a.	1840	FITC
483	wt	um	tris12	82.9	10.1	n.a.	1801	FITC
484	wt	um	del13p	9.6	12.8	84.4	2508	FITC
485	mut	m	norm	1.0	26.1	n.a.	1189	FITC
486	wt	um	norm	30.5	56.9	n.a.	1957	FITC
487	wt	um	del13p	97.5	70.2	45.3	2077	FITC
488	wt	um	tris12	53.4	64.5	n.a.	1801	FITC
489	wt	m	tris12	52.7	10.0	n.a.	9933	FITC
490	wt	m	norm	2.1	3.1	n.a.	1448	FITC
491	wt	m	del13p	71.8	29.4	n.a.	5602	FITC
492	wt	n.a.	del13p	54.3	56.3	n.a.	4293	FITC
493	wt	m	tris12	100.0	3.9	n.a.	13955	FITC
494	mut	um	del11q	94.7	18.0	n.a.	1610	FITC
495	wt	m	del13p	26.6	0.6	n.a.	2898	FITC
496	wt	m	del13p	1.5	1.2	n.a.	4453	PE-Cy7
497	wt	m	norm	1.9	1.0	n.a.	4904	PE-Cy7
498	wt	n.a.	del13p	1.0	1.0	n.a.	959	PE-Cy7
499	wt	n.a.	tris12	99.6	1.9	11.3	22455	PE-Cy7
500	wt	m	norm	10.3	26.8	41.5	8126	PE-Cy7
501	wt	um	norm	49.1	13.7	69.6	14052	PE-Cy7
502	wt	um	del13p	4.2	54.0	45.2	9527	PE-Cy7
503	mut	n.a.	norm	97.4	52.8	53.0	2488	PE-Cy7
504	wt	um	norm	1.0	2.9	34.2	7911	PE-Cy7
505	wt	m	del17p	100.0	97.0	16.1	39672	PE-Cy7
506	wt	m	del13p	1.3	1.8	19.8	15308	PE-Cy7
507	mut	m	del13p	82.1	91.4	35.2	10048	PE-Cy7
508	wt	um	norm	79.2	74.2	n.a.	11312	PE-Cy7
509	wt	um	tris12	74.4	37.3	85.4	15872	PE-Cy7
510	wt	n.a.	norm	99.5	26.7	29.3	98223	PE-Cy7
511	mut	um	del13p	18.5	8.4	18.3	10129	PE-Cy7
512	wt	um	norm	1.4	41.4	17.0	10522	PE-Cy7
513	wt	n.a.	del17p	99.7	3.3	10.5	59072	PE-Cy7
514	wt	n.a.	del13p	66.8	61.0	12.0	18593	PE-Cy7
515	wt	n.a.	del13p	99.8	11.9	56.6	5953	PE-Cy7

516	mut	um	tris12	2.5	18.4	55.8	9289	PE-Cy7
517	mut	m	del13p	1.0	1.0	29.0	9440	PE-Cy7
518	wt	n.a.	tris12	99.1	96.5	44.2	15799	PE-Cy7
519	wt	m	norm	9.0	25.6	11.1	1750	PE-Cy7
520	wt	m	norm	8.4	4.5	15.4	2797	PE-Cy7
521	wt	n.a.	del13p	1.0	14.6	n.a.	14631	PE-Cy7
522	wt	m	norm	1.0	1.0	n.a.	6310	PE-Cy7
523	wt	um	del17p	98.1	90.1	n.a.	17194	PE-Cy7
524	wt	um	norm	3.6	11.7	53.0	22052	PE-Cy7
525	wt	um	del11q	1.4	90.1	n.a.	16199	PE-Cy7
526	wt	m	norm	2.6	3.2	n.a.	11072	PE-Cy7
527	wt	um	del13p	1.0	9.1	n.a.	11323	PE-Cy7
528	wt	um	norm	4.9	4.5	n.a.	2669	PE-Cy7
529	wt	m	norm	98.4	95.0	n.a.	34450	PE-Cy7
530	wt	m	norm	99.9	22.5	n.a.	39517	PE-Cy7
531	wt	um	tris12	31.9	26.3	n.a.	21892	PE-Cy7
532	wt	um	del11q	99.4	99.5	n.a.	127823	PE-Cy7
533	mut	m	norm	66.2	35.2	n.a.	5049	PE-Cy7
534	wt	m	del13p	75.7	11.3	n.a.	16042	PE-Cy7
535	wt	m	del13p	74.1	1.4	n.a.	3635	PE-Cy7
536	wt	um	tris12	99.9	95.5	n.a.	13872	PE-Cy7
537	wt	v	del11q	0.6	72.9	n.a.	2284	PE-Cy7
538	wt	m	norm	100.0	4.3	n.a.	106070	PE-Cy7
539	wt	m	del13p	1.9	2.6	n.a.	8613	PE-Cy7
540	wt	um	del11q	70.0	23.7	n.a.	11791	PE-Cy7
541	wt	n.a.	del13p	20.2	76.2	n.a.	7392	PE-Cy7
542	wt	m	del13p	1.4	5.8	n.a.	17024	PE-Cy7
543	wt	m	norm	99.9	3.4	9.1	78446	PE-Cy7
544	wt	n.a.	del11q	1.0	3.5	10.6	4893	PE-Cy7
545	wt	um	del11q	24.6	32.9	19.1	3258	PE-Cy7
546	wt	um	del17p	95.0	3.0	3.4	235	PE-Cy7
547	wt	m	del13p	41.6	1.0	1.9	216	PE-Cy7
548	wt	n.a.	tris12	94.3	6.2	3.3	44201	PE-Cy7
549	wt	n.a.	del13p	1.0	1.0	3.5	15223	PE-Cy7
550	wt	m	del13p	1.0	4.6	2.7	6783	PE-Cy7
551	wt	n.a.	del13p	99.4	9.5	1.5	50671	PE-Cy7
552	wt	um	del11q	1.0	37.5	2.7	2538	PE-Cy7
553	wt	n.a.	del13p	1.1	17.6	10.1	10884	PE-Cy7
554	wt	n.a.	del13p	1.0	52.8	2.8	2967	PE-Cy7
555	mut	um	norm	65.5	33.7	30.0	7868	PE-Cy7
556	mut	n.a.	tris12	99.2	94.7	13.9	10616	PE-Cy7
557	wt	m	del13p	87.8	73.8	3.4	37919	PE-Cy7
558	mut	um	del13p	1.0	30.8	2.6	6321	PE-Cy7
559	wt	n.a.	del17p	61.5	5.7	4.7	138	PE-Cy7
560	wt	m	del13p	5.9	3.0	24.4	13792	PE-Cy7
561	wt	m	del13p	1.1	2.6	1.1	16848	PE-Cy7
562	wt	m	tris12	91.7	41.9	12.1	24078	PE-Cy7
563	wt	n.a.	norm	27.1	99.9	7.4	8984	PE-Cy7
564	wt	um	del11q	10.1	99.9	26.7	2803	PE-Cy7
565	wt	n.a.	del17p	34.7	99.0	35.7	49597	PE-Cy7
566	wt	m	tris12	98.6	97.9	5.7	8988	PE-Cy7
567	wt	m	del13p	2.9	98.4	14.1	18861	PE-Cy7

568	wt	m	del13p	1.0	72.4	7.0	6528	PE-Cy7
569	wt	m	norm	19.4	92.2	12.1	3264	PE-Cy7
570	wt	m	norm	9.2	1.6	17.2	12473	PE-Cy7
571	wt	um	del17p	96.5	7.4	44.3	1306	PE-Cy7
572	wt	m	norm	1.0	40.0	28.1	8647	PE-Cy7
573	mut	m	norm	1.4	10.4	4.4	4591	PE-Cy7
574	wt	n.a.	tris12	99.9	78.5	5.1	63037	PE-Cy7
575	wt	m	del13p	2.7	n.a.	11.3	11217	PE-Cy7
576	wt	m	del13p	1.0	4.6	5.2	8394	PE-Cy7
577	mut	n.a.	del11q	1.6	78.9	8.9	670	PE-Cy7
578	mut	n.a.	del11q	97.4	67.9	58.5	6489	PE-Cy7
579	wt	um	del11q	2.0	43.5	22.8	3618	PE-Cy7
580	wt	m	norm	16.1	n.a.	10.9	12370	PE-Cy7
581	wt	m	del13p	11.6	45.5	25.8	18932	PE-Cy7
582	wt	m	norm	5.8	86.6	15.0	8655	PE-Cy7
583	mut	um	tris12	75.3	n.a.	49.8	31190	PE-Cy7
584	wt	um	del13p	59.2	86.5	20.3	8070	PE-Cy7
585	wt	um	norm	78.4	24.2	23.0	9138	PE-Cy7
586	wt	m	del17p	1.3	1.8	6.2	10245	PE-Cy7
587	wt	n.a.	del17p	92.7	70.2	29.5	20123	PE-Cy7
588	wt	n.a.	del13p	6.8	0.7	3.0	5792	PE-Cy7
589	wt	n.a.	norm	99.6	98.1	55.1	16288	PE-Cy7
590	wt	um	del11q	1.7	56.7	13.9	6914	PE-Cy7
591	wt	m	del13p	3.8	1.0	9.1	9489	PE-Cy7
592	wt	m	del13p	1.2	1.0	10.9	13551	PE-Cy7
593	wt	um	del17p	64.8	82.5	43.8	17097	PE-Cy7
594	wt	m	del13p	97.7	20.8	1.0	81009	PE-Cy7
595	wt	m	del13p	100.0	11.9	54.8	34833	PE-Cy7
596	mut	m	del13p	2.6	1.2	1.0	4295	PE-Cy7
597	wt	n.a.	del13p	21.2	2.0	1.8	5091	PE-Cy7
598	wt	um	norm	58.8	35.9	41.7	3631	PE-Cy7
599	wt	m	del11q	1.0	9.9	11.6	5841	PE-Cy7
600	wt	um	del13p	5.4	20.6	5.3	4926	PE-Cy7
601	wt	um	norm	58.7	92.3	60.8	10400	PE-Cy7
602	wt	um	del17p	78.0	51.3	47.3	6142	PE-Cy7
603	wt	n.a.	norm	27.0	1.5	7.3	6029	PE-Cy7
604	wt	um	del17p	12.6	53.4	15.4	5061	PE-Cy7
605	wt	m	norm	26.2	0.8	0.4	3330	PE-Cy7
606	wt	m	norm	8.4	1.2	6.4	5290	PE-Cy7
607	wt	m	del13p	1.2	0.7	0.7	8898	PE-Cy7
608	mut	um	del13p	23.2	50.7	17.0	10661	PE-Cy7
609	wt	um	del11q	84.0	80.4	8.1	4689	PE-Cy7
610	wt	m	norm	3.2	2.1	5.6	25972	PE-Cy7
611	mut	um	del13p	93.4	62.8	36.6	15569	PE-Cy7
612	mut	n.a.	tris12	91.7	96.1	53.8	9559	PE-Cy7
613	wt	n.a.	norm	91.3	82.7	5.7	15850	PE-Cy7
614	wt	m	del13p	3.8	8.7	4.7	5326	PE-Cy7
615	wt	um	del11q	23.4	36.5	5.3	5414	PE-Cy7
616	wt	m	norm	64.4	5.4	11.5	70994	PE-Cy7
617	wt	n.a.	tris12	99.6	43.7	7.0	81891	PE-Cy7
618	wt	n.a.	del13p	2.0	4.6	15.4	16932	PE-Cy7
619	wt	m	tris12	97.9	73.1	4.1	34618	PE-Cy7

620	wt	n.a.	norm	6.2	51.1	3.2	9245	PE-Cy7
621	wt	m	del13p	3.7	1.0	2.4	18710	PE-Cy7
622	mut	um	del13p	99.6	88.3	22.3	23782	PE-Cy7
623	mut	v	del11q	2.3	39.8	11.9	5392	PE-Cy7
624	mut	m	del13p	2.0	6.0	27.3	8882	PE-Cy7
625	wt	n.a.	norm	12.2	4.2	21.5	10916	PE-Cy7
626	wt	m	norm	15.5	2.0	2.9	5888	PE-Cy7
627	mut	um	tris12	70.9	33.9	8.0	7433	PE-Cy7
628	wt	m	del17p	74.7	45.2	1.0	6898	PE-Cy7
629	wt	n.a.	del13p	1.0	57.7	37.1	18016	PE-Cy7
630	wt	um	norm	2.7	85.7	n.a.	11081	PE-Cy7
631	mut	um	tris12	92.1	78.9	n.a.	9469	PE-Cy7
632	wt	um	del11q	1.4	18.3	21.7	15183	PE-Cy7
633	wt	m	norm	4.6	3.9	n.a.	5935	PE-Cy7
634	wt	n.a.	tris12	2.4	16.2	n.a.	11297	PE-Cy7
635	wt	m	del13p	21.7	0.6	n.a.	9792	PE-Cy7
636	wt	m	norm	57.0	1.5	22.1	12493	PE-Cy7
637	wt	um	del11q	8.5	63.0	3.8	7734	PE-Cy7
638	wt	um	del11q	4.1	3.8	12.5	8890	PE-Cy7
639	mut	n.a.	norm	99.5	74.7	32.0	4200	PE-Cy7
640	mut	um	norm	1.4	37.0	9.1	18892	PE-Cy7
641	wt	n.a.	del17p	17.6	2.9	9.9	8044	PE-Cy7
642	wt	n.a.	norm	4.0	1.3	7.0	4065	PE-Cy7
643	wt	m	del13p	10.1	1.0	2.8	33304	PE-Cy7
644	wt	m	tris12	100.0	16.7	6.7	55877	PE-Cy7
645	wt	um	del13p	0.3	0.9	3.8	10629	PE-Cy7
646	wt	um	norm	5.3	49.5	6.9	6771	PE-Cy7
647	wt	um	tris12	88.3	30.3	44.2	15432	PE-Cy7
648	wt	um	norm	85.0	14.0	14.4	8514	PE-Cy7
649	wt	m	norm	2.1	1.4	4.6	2576	PE-Cy7
650	wt	m	del13p	1.6	1.4	3.5	5288	PE-Cy7
651	mut	um	del13p	50.4	2.3	15.2	7024	PE-Cy7
652	wt	um	del13p	95.9	97.5	39.8	5373	PE-Cy7
653	wt	um	del13p	74.6	44.4	19.8	5479	PE-Cy7
654	wt	m	tris12	44.2	42.2	10.8	6760	PE-Cy7
655	wt	m	del13p	3.2	4.6	11.3	22589	PE-Cy7
656	wt	m	del13p	0.8	1.1	17.9	12746	PE-Cy7
657	wt	m	norm	36.9	2.7	17.9	12462	PE-Cy7
658	wt	um	norm	70.0	14.8	34.8	6127	PE-Cy7
659	wt	um	del11q	1.7	76.2	13.8	9661	PE-Cy7
660	wt	n.a.	norm	25.5	3.5	6.3	5571	PE-Cy7
661	wt	n.a.	del17p	51.5	n.a.	n.a.	12086	PE-Cy7
662	wt	n.a.	tris12	59.9	33.7	19.5	34358	PE-Cy7
663	wt	m	del13p	100.0	5.3	26.7	63749	PE-Cy7
664	wt	m	del13p	0.9	1.7	37.7	12327	PE-Cy7
665	wt	m	del13p	2.4	1.8	50.0	15916	PE-Cy7
666	wt	n.a.	tris12	87.5	44.0	42.5	9258	PE-Cy7
667	wt	um	norm	99.8	76.6	68.8	16479	PE-Cy7
668	wt	um	norm	99.0	73.3	34.0	6195	PE-Cy7
669	wt	um	del13p	19.6	20.2	10.1	20026	PE-Cy7
670	wt	m	del13p	93.4	2.3	5.9	11419	PE-Cy7
671	wt	m	del13p	2.2	1.3	7.0	20704	PE-Cy7

672	wt	n.a.	del11q	3.5	96.9	11.9	3934	PE-Cy7
673	wt	m	del13p	1.2	2.0	9.0	15115	PE-Cy7
674	wt	m	del17p	68.4	53.3	21.9	9478	PE-Cy7
675	mut	n.a.	norm	27.5	7.9	9.8	19007	PE-Cy7
676	wt	um	del13p	1.4	1.4	n.a.	20411	PE-Cy7
677	wt	um	del13p	1.0	2.6	n.a.	1921	PE-Cy7
678	wt	um	del13p	3.2	6.5	n.a.	760	PE-Cy7
679	wt	n.a.	del17p	92.7	70.2	n.a.	31757	PE-Cy7
680	wt	n.a.	del11q	90.0	58.4	n.a.	4446	PE-Cy7
681	wt	n.a.	del13p	2.7	6.0	7.0	4602	PE-Cy7
682	wt	um	del11q	0.8	8.0	3.2	5824	PE-Cy7
683	wt	m	del13p	2.0	4.2	1.2	6989	PE-Cy7
684	wt	m	del17p	2.2	12.2	8.7	18510	PE-Cy7
685	wt	um	del11q	89.1	99.7	12.7	7069	PE-Cy7
686	wt	m	del13p	10.7	16.4	20.3	16968	PE-Cy7
687	wt	n.a.	del13p	0.2	2.4	44.7	19062	PE-Cy7
688	wt	um	del11q	70.0	0.5	44.9	13701	PE-Cy7
689	wt	m	del13p	1.8	0.6	13.2	16881	PE-Cy7
690	wt	m	del13p	0.7	14.9	16.1	8071	PE-Cy7
691	wt	m	del13p	0.7	0.5	8.1	6223	PE-Cy7
692	mut	um	norm	60.3	64.6	15.3	17759	PE-Cy7

a: as determined by ARMS-PCR, conventional and next-generation sequencing.
b: *IGHV* status was established according to the conventional cut-off, as reported in ref. 28.
c: FISH status was determined according to ref. 38.
d: CD49d, CD38 and ZAP70 expression are reported as percentage of positive cells.
e: ZAP70 expression was determined as reported in ref. 28.
f: MFI values are substracted from the values of irrelevant isotype-matched antibody.
g: the type of fluorochrome utilized to determine CD20 expression is reported.

Abbreviations: ID #: identification number, *NOTCH1* status: wt, *NOTCH1* wild type, mut, *NOTCH1* mutated; *IGHV* status: um, *IGHV* unmutated, m, *IGHV* mutated; FISH: norm, normal karyotype; n.a., not available.

Table S2. *NOTCH1* mutation features of the *NOTCH1* mutated cohort (87 cases).

ID #	% of mutated DNA[a,b]	Mutation
2	40	c.7541-7542delCT p.2514fs*4; c.7426G>A p.V2477M
4	15	c.7541-7542delCT p.2514fs*4
26	6	c.7541-7542delCT p.2514fs*4
34	8	c.7541-7542delCT p.2514fs*4
48	36	c.7541-7542delCT p.2514fs*4
53	25[b]	c.7293delG p.R2431fs*4
62	31	c.7541-7542delCT p.2514fs*4
75	5	c.7541-7542delCT p.2514fs*4
78	35	c.7541-7542delCT p.2514fs*4
95	13	c.7541-7542delCT p.2514fs*4
97	4	c.7541-7542delCT p.2514fs*4
103	43	c.7541-7542delCT p.2514fs*4
104	25-50[b]	c.7264delG p.V2422fs*1
105	41	c.7541-7542delCT p.2514fs*4
107	1	c.7541-7542delCT p.2514fs*4
113	50[b]	c.6823-6824delTC p.S2275fs*79
120	13	c.7541-7542delCT p.2514fs*4
122	23	c.7541-7542delCT p.2514fs*4
139	16	c.7541-7542delCT p.2514fs*4
144	40	c.7541-7542delCT p.2514fs*4
146	5	c.7541-7542delCT p.2514fs*4
147	39	c.7541-7542delCT p.2514fs*4
163	1	c.7541-7542delCT p.2514fs*4
170	1	c.7541-7542delCT p.2514fs*4
171	27	c.7541-7542delCT p.2514fs*4
173	6	c.7541-7542delCT p.2514fs*4
175	32	c.7541-7542delCT p.2514fs*4
176	31	c.7541-7542delCT p.2514fs*4
185	1	c.7541-7542delCT p.2514fs*4
191	31	c.7541-7542delCT p.2514fs*4
214	24	c.7541-7542delCT p.2514fs*4
218	1	c.7541-7542delCT p.2514fs*4
224	1	c.7541-7542delCT p.2514fs*4
233	2	c.7541-7542delCT p.2514fs*4
243	35	c.7541-7542delCT p.2514fs*4
244	50	c.7541-7542delCT p.2514fs*4
264	31	c.7541-7542delCT p.2514fs*4
266	41	c.7541-7542delCT p.2514fs*4
269	34	c.7541-7542delCT p.2514fs*4
298	38	c.7541-7542delCT p.2514fs*4
303	<25[b]	c.7330C>T p.Q2445*
304	4	c.7541-7542delCT p.2514fs*4
305	26	c.7541-7542delCT p.2514fs*4
340	15	c.7541-7542delCT p.2514fs*4
347	1	c.7541-7542delCT p.2514fs*4
365	25[b]	c.7330C>T p.Q2445*
369	24	c.7541-7542delCT p.2514fs*4
379	13	c.7541-7542delCT p.2514fs*4
383	8	c.7541-7542delCT p.2514fs*4
406	2	c.7541-7542delCT p.2514fs*4

408	11	c.7541-7542delCT p.2514fs*4
420	2	c.7541-7542delCT p.2514fs*4
428	25-50[b]	c.6460C>T p.Q2154*
431	41	c.7541-7542delCT p.2514fs*4
442	22	c.7541-7542delCT p.2514fs*4
458	1	c.7541-7542delCT p.2514fs*4
461	2	c.7541-7542delCT p.2514fs*4
476	15	c.7541-7542delCT p.2514fs*4
485	1	c.7541-7542delCT p.2514fs*4
494	2	c.7541-7542delCT p.2514fs*4
503	15	c.7541-7542delCT p.2514fs*4
507	27	c.7541-7542delCT p.2514fs*4
511	15	c.7541-7542delCT p.2514fs*4
516	5	c.7541-7542delCT p.2514fs*4
517	8	c.7541-7542delCT p.2514fs*4
533	1	c.7541-7542delCT p.2514fs*4
555	12	c.7541-7542delCT p.2514fs*4
556	4	c.7541-7542delCT p.2514fs*4
558	1	c.7541-7542delCT p.2514fs*4
573	1	c.7541-7542delCT p.2514fs*4
577	5	c.7541-7542delCT p.2514fs*4
578	4	c.7541-7542delCT p.2514fs*4
583	4	c.7541-7542delCT p.2514fs*4
596	3	c.7541-7542delCT p.2514fs*4
608	4	c.7541-7542delCT p.2514fs*4
611	42	c.7541-7542delCT p.2514fs*4
612	11	c.7541-7542delCT p.2514fs*4
622	3	c.7541-7542delCT p.2514fs*4
623	1	c.7541-7542delCT p.2514fs*4
624	3	c.7541-7542delCT p.2514fs*4
627	7	c.7541-7542delCT p.2514fs*4
631	6	c.7541-7542delCT p.2514fs*4
639	2	c.7541-7542delCT p.2514fs*4
640	2	c.7541-7542delCT p.2514fs*4
651	1	c.7541-7542delCT p.2514fs*4
675	3	c.7541-7542delCT p.2514fs*4
692	39	c.7541-7542delCT p.2514fs*4

a: the reported values are rounded up to the whole number.

b: mutational load was determined by visual scrutiny of sequence electopherograms as in ref.31 .

c: as determined by Sanger sequencing.

Abbreviations: ID#: identification number.

Supplementary Figure Legends

Figure S1. NOTCH1 transmembrane and NICD protein expression in *NOTCH1*-mut and *NOTCH1*-wt CLL cases. NOTCH1 transmembrane (NOTCH1-TM, upper panel) and NICD (lower panel) protein expression in 7 *NOTCH1*-wt and 4 *NOTCH1*-mut CLL cases, as evaluated by WB. β-actin was used as loading control. "Short" indicates short exposure.

Figure S2. CD20 expression levels in CLL cells (first series) and in normal B cells from healthy donors. **(a)** Box-and-whiskers plots showing CD20 protein expression levels, in CLL cells from a series of 495 CLL cases, according to cytogenetic abnormalities, and in the residual normal B cell (i.e. $CD19^+$ $CD5^-$) components, as evaluated by flow cytometry using a FITC-conjugated anti-CD20 antibody. **(b)** Dot plot showing CD20 expression, as evaluated by flow cytometry using a FITC-conjugated anti-CD20 antibody, in prototypic *NOTCH1*-mut and *NOTCH1*-wt cases of trisomy 12 and non-trisomy 12 CLL categories.

Figure S3. CD20 expression levels in CLL cells (second series), divided according to cytogenetic abnormalities. (a) Box-and-whiskers plots showing CD20 protein expression levels in CLL cells from a series of 197 CLL cases, according to cytogenetic abnormalities, as evaluated by flow cytometry using a PE-Cy7-conjugated anti-CD20 antibody. **(b)** Box-and-whiskers plots showing CD20 protein expression levels, as evaluated by flow cytometry with a PE-Cy7-conjugated anti-CD20 antibody, in 23 trisomy 12 CLL cases (6 *NOTCH1*-mut cases, 17 *NOTCH1*-wt cases) and in 174 non-trisomy 12 CLL cases (21 *NOTCH1*-mut cases, 153 *NOTCH1*-wt cases). The corresponding p values are reported.

Figure S4. Cell sorting of $CD20^{low}$ and $CD20^{high}$ subpopulations in *NOTCH1*-mut CLL cases. Dot plots representing the gating strategy of cell sorting experiments according to CD20 expression in 5 *NOTCH1*-mut CLL cases. The $CD20^{low}$ or $CD20^{high}$ fractions were selected below the 25^{th} percentile or above the 75^{th} percentile of CD20 expression, respectively.

Figure S5. Induction of CD20 expression by NOTCH1 signaling inhibition in *NOTCH1*-mut and *NOTCH1*-wt CLL cases. **(a)** Histograms showing *HES1* transcript fold change, upon GSI treatment for 6 hours, of *NOTCH1*-mut and *NOTCH1*-wt CLL cases, as evaluated by QRT-PCR. The corresponding p value is reported. **(b)** Box-and-whiskers plots showing *MS4A1* transcript expression levels of CLL cell samples, untreated (UNT) and GSI treated (GSI) for 6 hours, of *NOTCH1*-mut and *NOTCH1*-wt CLL cases, as evaluated by QRT-PCR. The corresponding p values are reported (upper panel). Dot-and-line diagrams showing CD20 expression levels of CLL cell samples, untreated (UNT) and GSI treated (GSI) for 24 hours, of *NOTCH1*-mut and *NOTCH1*-wt CLL cases, as evaluated by flow cytometry. The corresponding p values are reported (lower panel). **(c)** Dot-and-line diagrams showing NOTCH1 expression levels of CLL cell samples, transfected with scramble control (NC) and transfected with siRNA for NOTCH1 (siRNA) for 24 hours, of *NOTCH1*-mut and *NOTCH1*-wt CLL cases, as evaluated by flow cytometry. The corresponding p values are reported (upper panel). Dot-and-line diagrams showing CD20 expression levels of CLL cell samples, transfected with scramble control (NC) and transfected with siRNA for NOTCH1 (siRNA) for 24 hours, of *NOTCH1*-mut and *NOTCH1*-wt CLL cases, as evaluated by flow cytometry. The corresponding p values are reported (lower panel).

Figure S6. Loading controls for the RBPJ co-immunoprecipation. (a) Low exposure images of the immunoblotting reported as Figure 3a. HDAC1 and HDAC2 are equally expressed between NICD-mut and NICD-null transfectants. ISO: isotypic antibody; WNL: whole nuclear lysates. **(b)**

Immunoblotting of RBPJ, with a second antibody, in lysates derived from NICD-mut and NICD-null cells as shown in Figure 3a, i.e. whole nuclear (WNL), immunoprecipitates with isotypic control (ISO) and immunoprecipitates with RBPJ (RBPJ) itself. **(c)** Immunoblotting for NOTCH1, RBPJ, HDAC1 and HDAC2 of cytoplasmic (C) and nuclear (N) lysates from NICD-mut and NICD-null transfectants. ERK1/2 was used as cytoplasmic control. BRG-1 was used as nuclear control.

Figure S7. Constitutive *HDAC1* and *HDAC2* expression levels in *NOTCH1*-mut and *NOTCH1*-wt CLL cases. Box-and-whiskers plots showing constitutive *HDAC1* (left panel) and *HDAC2* (right panel) transcript expression levels of 275 CLL cases (46 *NOTCH1*-mut and 229 *NOTCH1*-wt cases), as evaluated by QRT-PCR. The corresponding p values are reported.

Figure S8. Induction of *MS4A1* transcript expression by HDAC inhibition in-vitro. (a) Box-and-whiskers plots showing *MS4A1* transcript expression levels of untreated (UNT) and VPA treated (VPA) cell samples for 48 hours of NICD-mut and NICD-null cells, as evaluated by QRT-PCR. The corresponding p values are reported. Results of three independent experiments are showed. **(b)** Box-and-whiskers plots showing *MS4A1* transcript expression levels of CLL cell samples, untreated (UNT) and VPA treated (VPA) for 48 hours, of *NOTCH1*-mut and *NOTCH1*-wt CLL cases, as evaluated by QRT-PCR. The corresponding p values are reported.

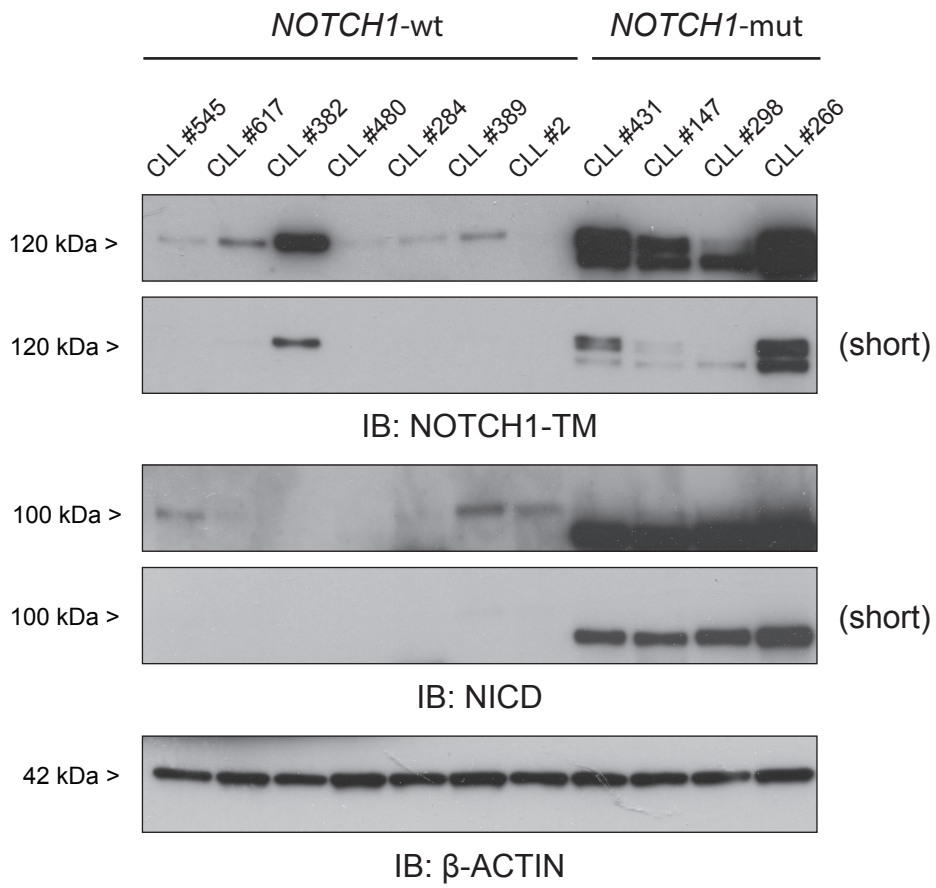
NOTCH1-wt
NOTCH1-mut
CLL #545
CLL #617
CLL #382
CLL #480
CLL #284
CLL #389
CLL #2
CLL #431
CLL #147
CLL #298
CLL #266
120 kDa >
120 kDa >
(short)
IB: NOTCH1-TM
100 kDa >
100 kDa >
(short)
IB: NICD
42 kDa >
IB: β-ACTIN

Figure S1

a

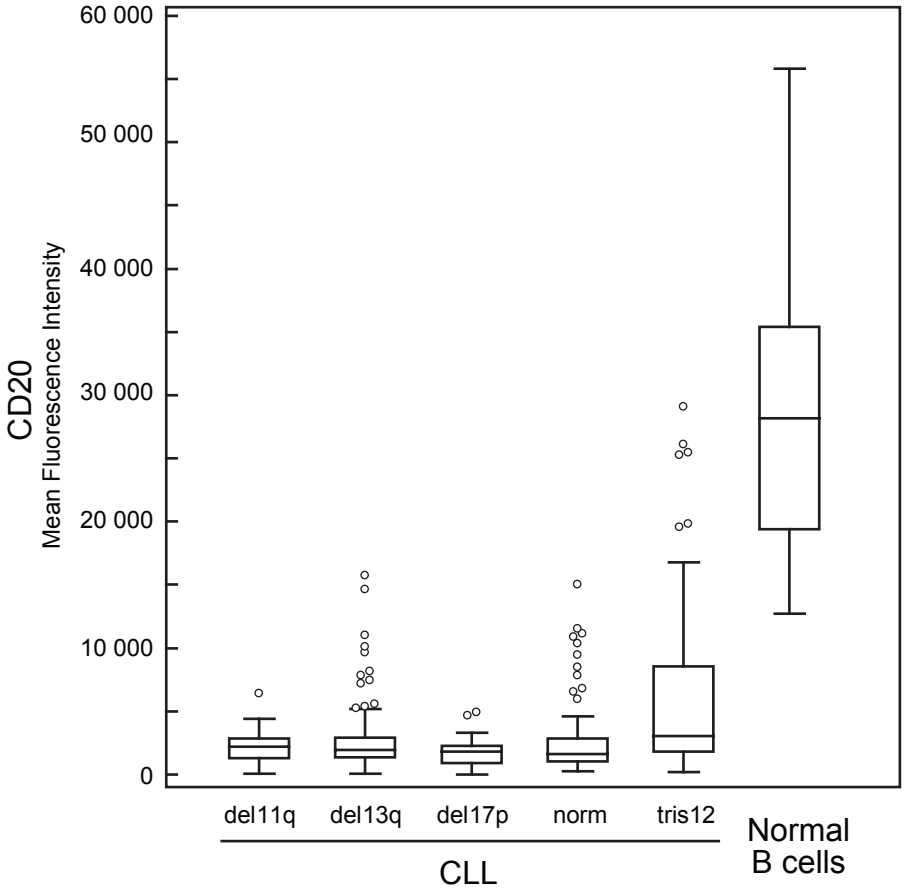
60 000
50 000
40 000
30 000
20 000
10 000
0
CD20
Mean Fluorescence Intensity
del11q
del13q
del17p
norm
tris12
CLL
Normal
B cells

b

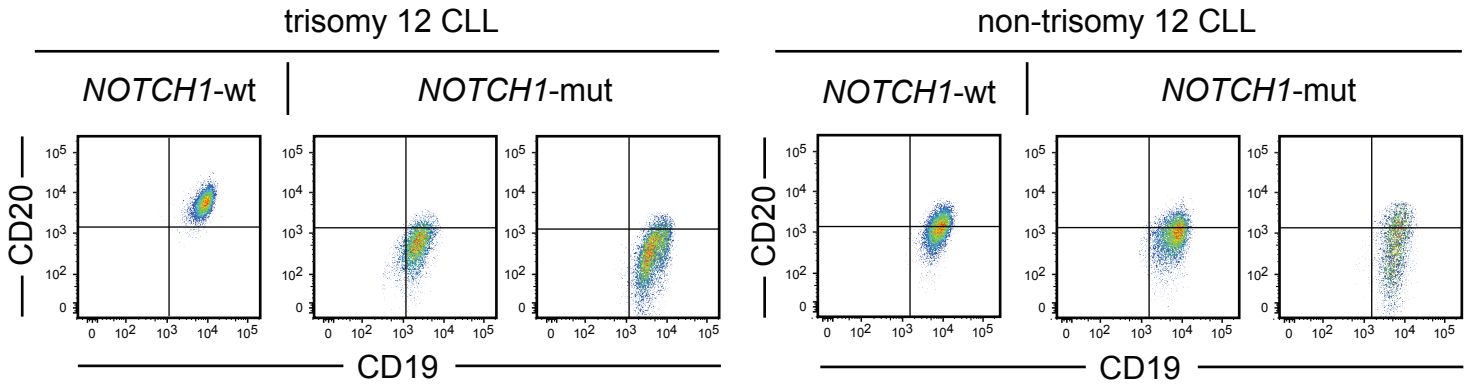
trisomy 12 CLL
non-trisomy 12 CLL
NOTCH1-wt
NOTCH1-mut
NOTCH1-wt
NOTCH1-mut
CD20
CD19
CD20
CD19

Figure S2

a

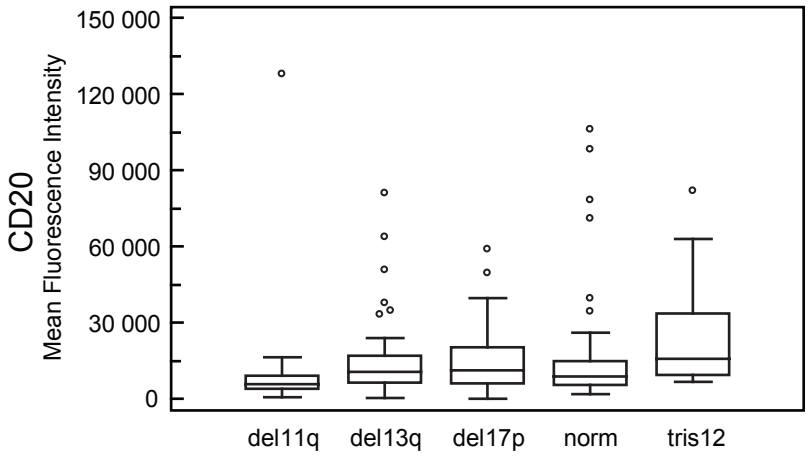
CD20
Mean Fluorescence Intensity
150 000
120 000
90 000
60 000
30 000
0
del11q
del13q
del17p
norm
tris12

b

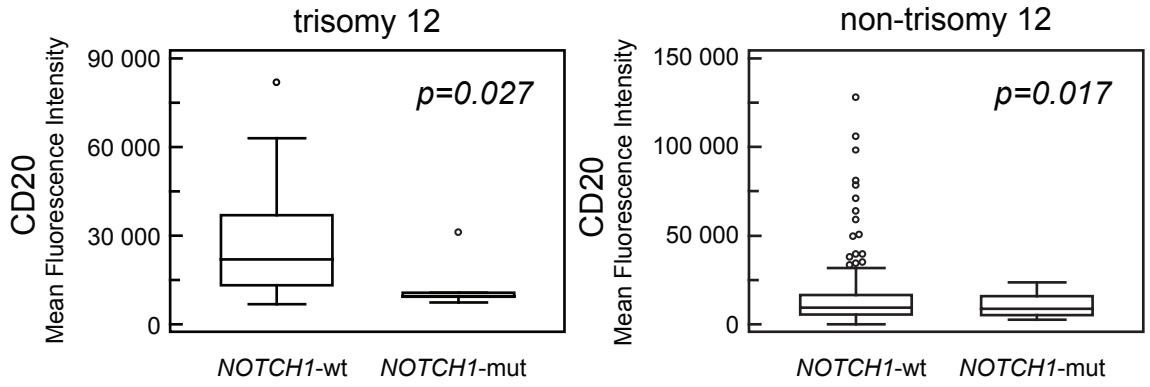
trisomy 12
CD20
Mean Fluorescence Intensity
90 000
60 000
30 000
0
p=0.027
NOTCH1-wt
NOTCH1-mut
non-trisomy 12
CD20
Mean Fluorescence Intensity
150 000
100 000
50 000
0
p=0.017
NOTCH1-wt
NOTCH1-mut

Figure S3

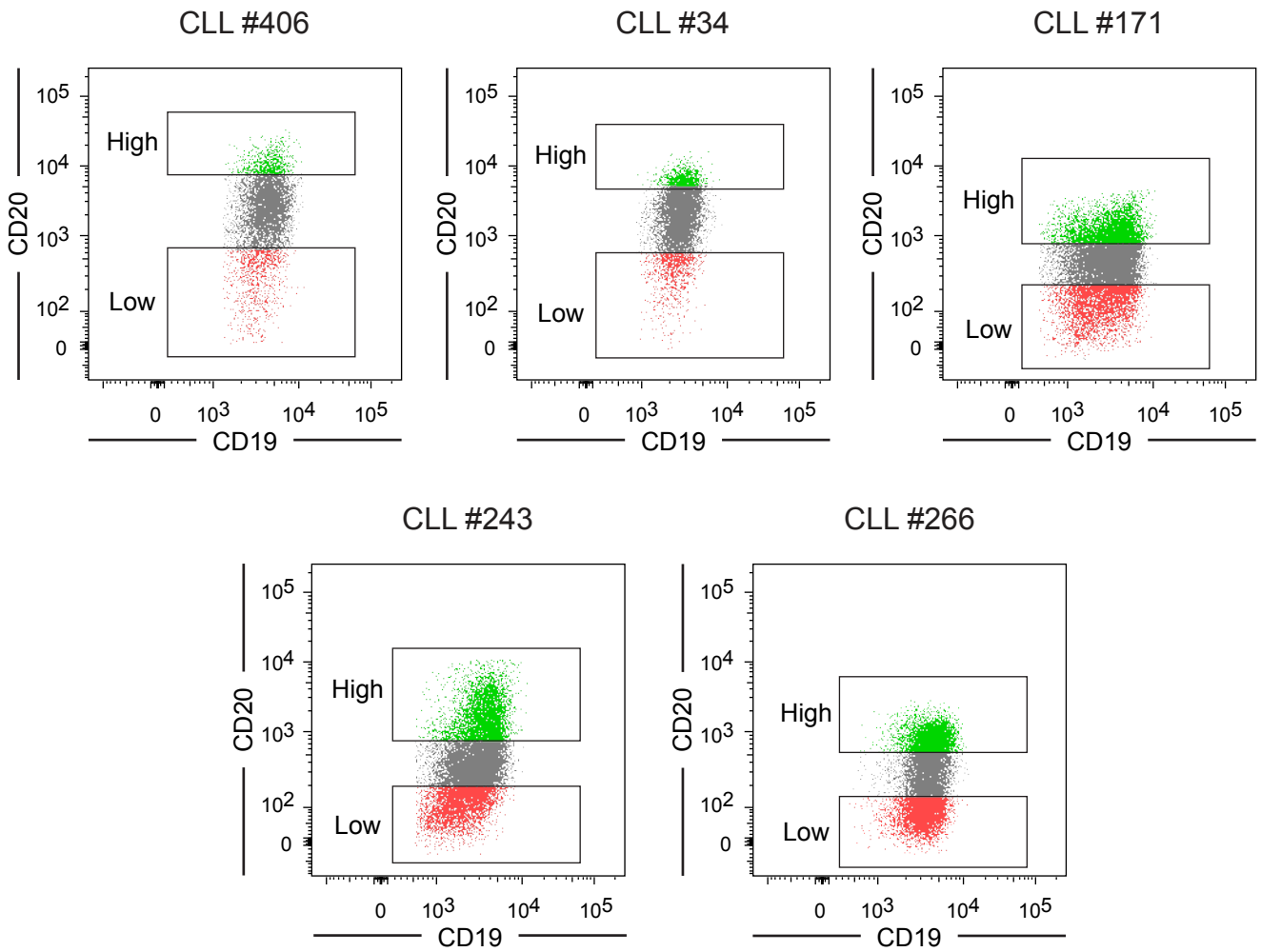
CLL #406
CLL #34
CLL #171
CLL #243
CLL #266
High
Low
CD20
CD19
0
10^2
10^3
10^4
10^5

Figure S4

a

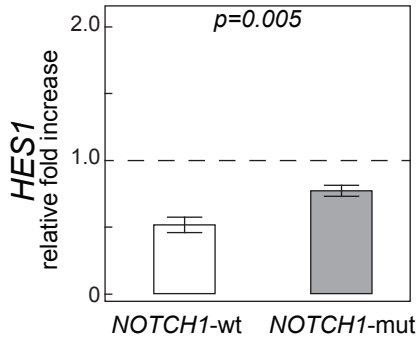

b

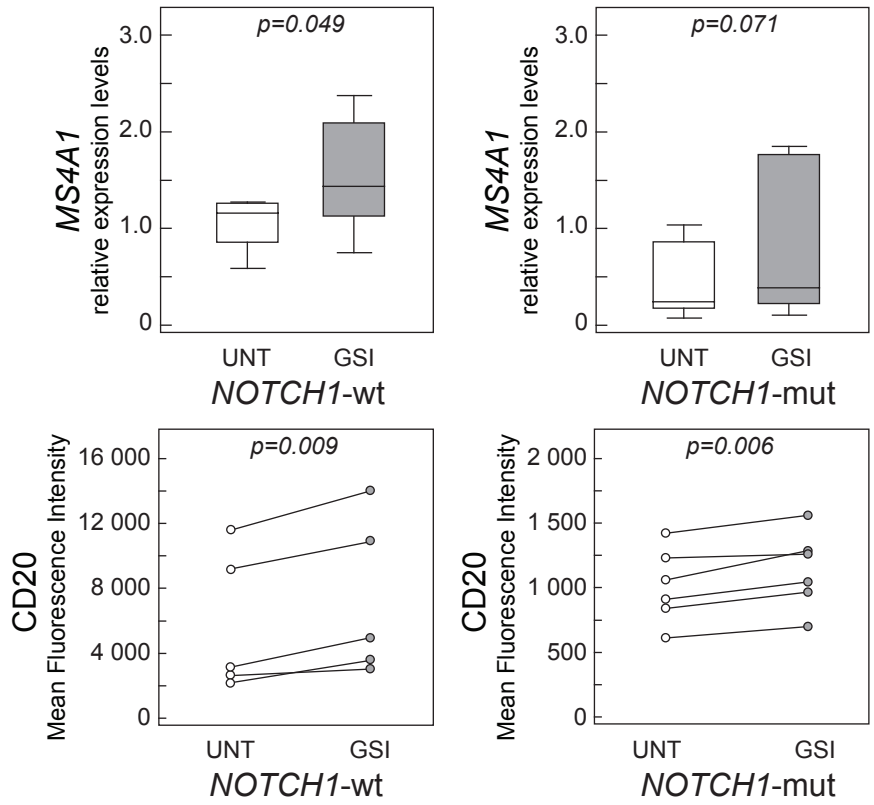

c

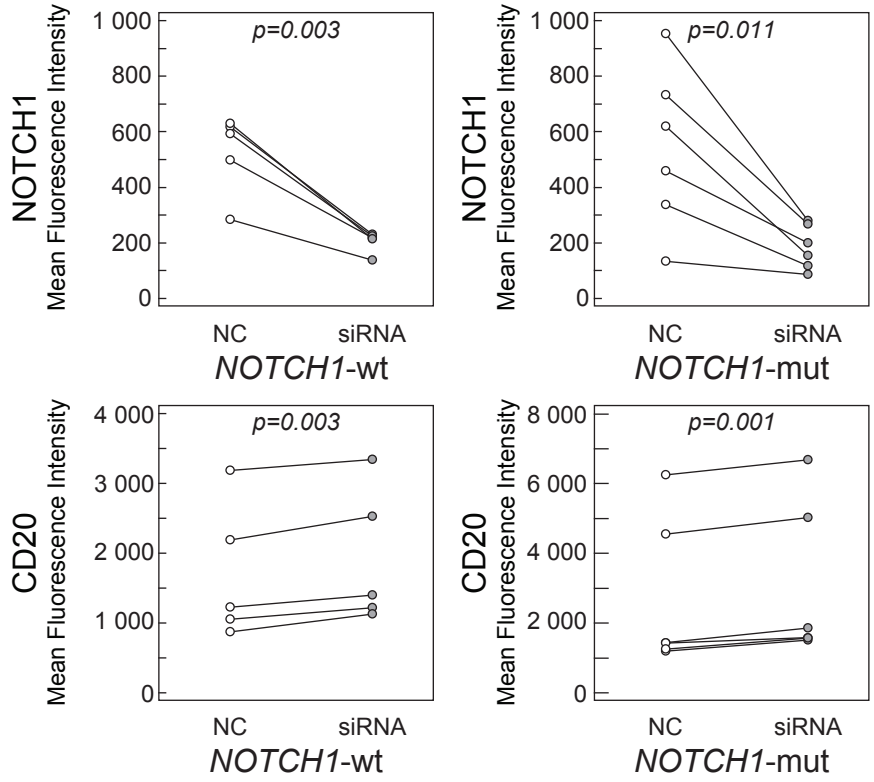

Figure S5

a

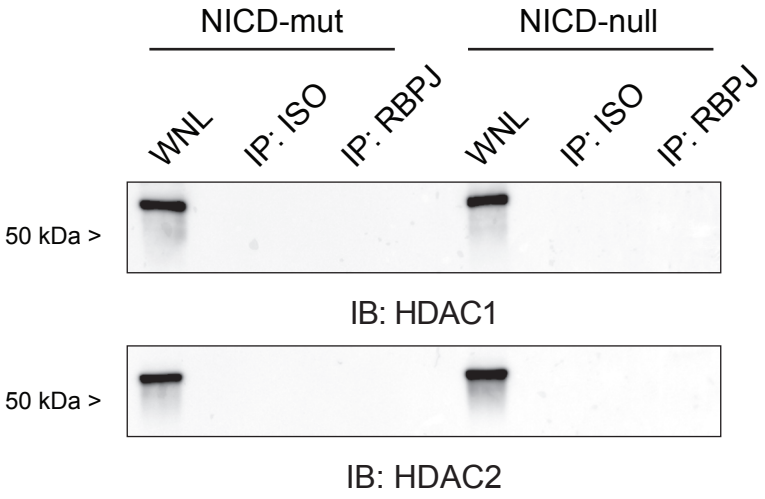

b

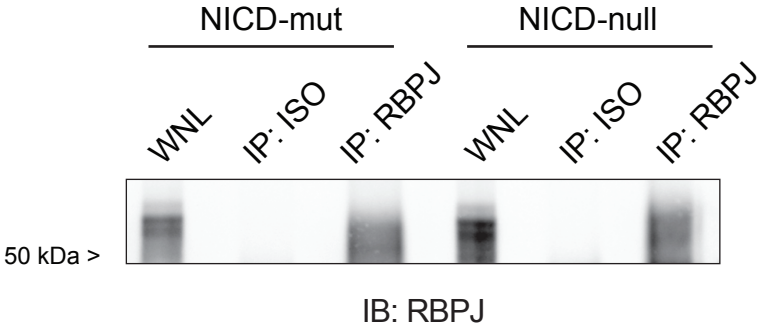

c

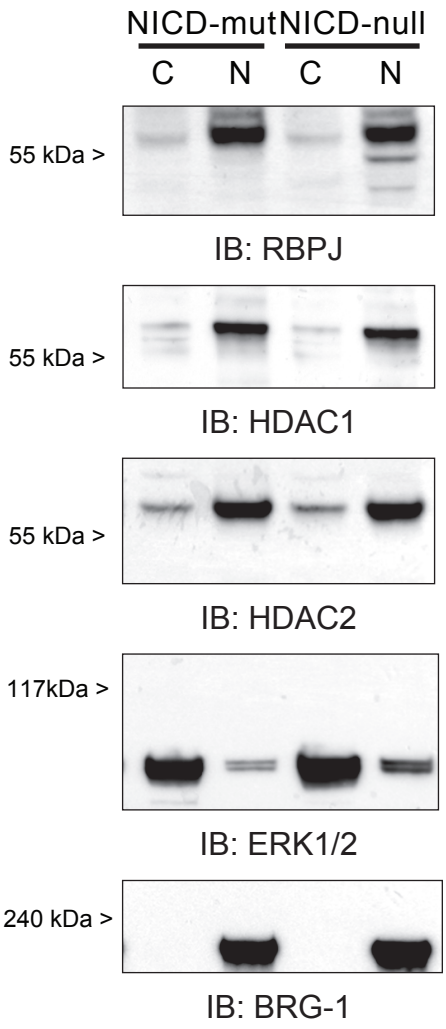

Figure S6

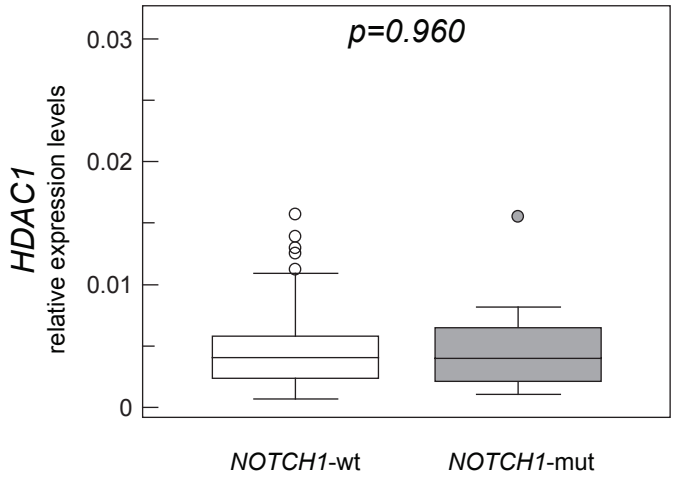
p=0.960
HDAC1
relative expression levels
0.03
0.02
0.01
0
NOTCH1-wt
NOTCH1-mut

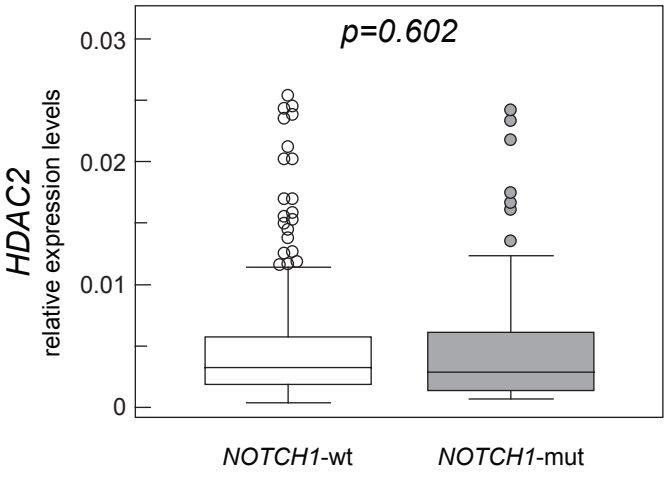
p=0.602
HDAC2
relative expression levels
0.03
0.02
0.01
0
NOTCH1-wt
NOTCH1-mut

Figure S7

a

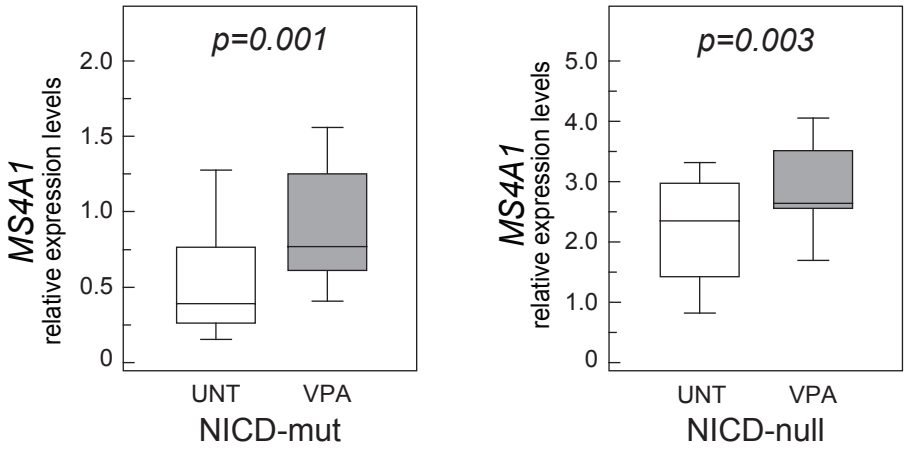
p=0.001
MS4A1
relative expression levels
2.0
1.5
1.0
0.5
0
UNT
VPA
NICD-mut
p=0.003
MS4A1
relative expression levels
5.0
4.0
3.0
2.0
1.0
0
UNT
VPA
NICD-null

b

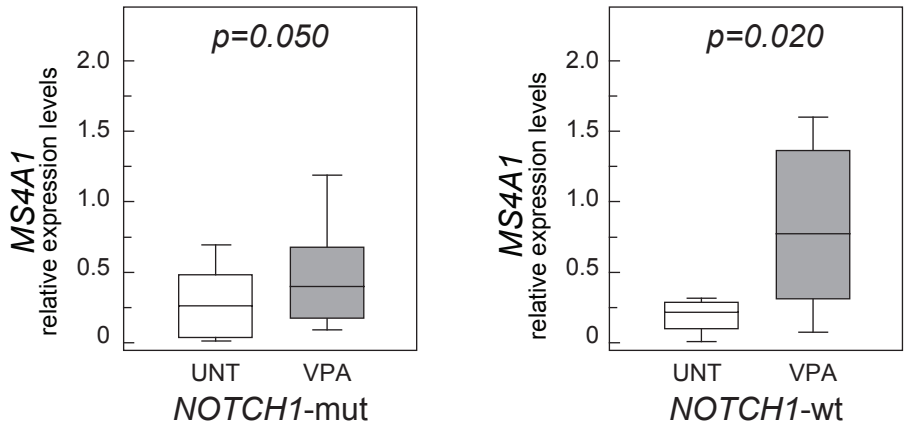
p=0.050
MS4A1
relative expression levels
2.0
1.5
1.0
0.5
0
UNT
VPA
NOTCH1-mut
p=0.020
MS4A1
relative expression levels
2.0
1.5
1.0
0.5
0
UNT
VPA
NOTCH1-wt

Figure S8